1	Cretaceous	(Albian-Turoni	an) calcareou	s nannofossil b	iostratigraph	y of the onshore

2 Cauvery Basin, southeastern India

Sudeep Kanungo^{a, b}*, Paul Bown^c, Andrew Gale^d

3

4

5

6

7

8

9

10

11

12

13

14

15

16

17

^a University of Utah, Energy & Geoscience Institute (EGI), 423 Wakara Way, Suite 300, Salt
Lake City, Utah 84108, USA
^b University of Utah, Dept. of Geology and Geophysics, Salt Lake City, Utah 84112, USA
° Dept. of Earth Sciences, University College London, Gower Street, London WC1E 6BT, UK
^d School of Earth & Environmental Sciences, University of Portsmouth, Burnaby Road,
Portsmouth PO1 3QL, UK
*Corresponding author: <u>skanungo@egi.utah.edu (Sudeep Kanungo)</u>
Abstract
A suite of outcrop samples from the Cauvery Basin belonging to the mudrock-claystone
dominated Karai Formation were analysed for nannofossil biostratigraphy in two newly
measured sections at Karai and Garudamangalam. The age of the Karai Section is interpreted as

18 early Albian to early Turonian, whereas the Garudamangalam Section is interpreted as late

19 Albian to late Cenomanian. The Albian 'BC' zones of Bown et al. (1998) are applicable in both

20 sections, whereas the Cenomanian and Turonian 'UC' zones of Burnett (1998), are only partially

21 applicable, due to some problematic primary and secondary markers. The Albian-Cenomanian

22 boundary appears to be continuous and is approximated in both sections using the FO of lower

23 Cenomanian ammonites of the M. mantelli Zone. The Cenomanian-Turonian boundary interval

24	is incomplete in the two sections, with a hiatus of ~ 0.66 Myr, indicated by the absence of the
25	upper Cenomanian Nannofossil Zone UC5. The nannoplankton assemblages are composed of
26	broadly cosmopolitan taxa, despite the relatively high-latitude setting of SE India during the
27	Albian (~45°S), which is reflected in the common occurrence of biogeographically bipolar taxa
28	such as Repagulum parvidentatum and Seribiscutum primitivum. The palaeobiogeographic
29	affinity of the nannoplankton, however, does not bear a distinct Austral stamp, as typical Austral
30	taxa, such as Sollasites falklandensis and Zeugrhabdotus kerguelenensis are very rare in the
31	studied sections. The early appearance of Crucibiscutum hayi in the lower Albian, and
32	Gartnerago segmentatum in the upper Albian in the Cauvery Basin suggests that these two
33	species may have originated in southern high latitudes before migrating to the northern Boreal
34	regions. Four new calcareous nannofossil species, Calculites karaiensis, Loxolithus bicyclus,
35	Manivitella fibrosa and Tranolithus simplex are described.
36	
37	Highlights
38	• A high-resolution Albian-Turonian biostratigraphy is established for the Cauvery Basin
39	using integrated calcareous nannofossil and ammonite data.
40	• The FO of <i>G. ponticula</i> is proposed as a new nannofossil proxy for approximating the
41	Albian-Cenomanian boundary.
40	

- A Cenomanian-Turonian boundary interval hiatus equivalent to Nannofossil Zone UC5 is
 present, representing a magnitude of ~0.66 Myr.
- The Austral character of the Cauvery Basin nannoplankton assemblages is suppressed.
- 45

Keywords: Cretaceous, Nannofossils, Ammonites, Correlation, South India, Gondwana, Karai,
Garudamangalam, Palaeobiogeography, Austral

48

49 **1. Introduction**

50

51 The Cauvery Basin is an important Mesozoic depocentre of southern India and contains a 52 well-developed marine Cretaceous succession that is known for its palaeontological (micro- and 53 macrofossil) and lithological diversity. The basin is the southernmost among a series of NE-SW 54 trending pericratonic, passive-margin rift basins on the eastern Coromandel Coast of India (Fig. 55 1). It has a large areal extent (~25, 000 sq. km) covering much of Tamil Nadu state, and extends 56 into the shallow offshore area to the east (~30, 000 sq. km). The basin is known for commercial 57 hydrocarbon production and has a Cretaceous petroleum system in place (Govindan et al., 2000; 58 DGH, 2018). A more recent discovery in the Cretaceous by Reliance Industries Limited has 59 opened new avenues for exploration in the deep waters (~95, 000 sq. km) of the Cauvery Basin 60 (DGH, 2018).

61

The stratigraphy of the basin has been primarily worked out from outcrop geology and extended to the subsurface through drilled and seismic data (Govindan et al., 1996; Rao et al., 2010). This calls for improving stratigraphic constraints in the Cretaceous marine sedimentary successions in the basin that range from the Albian to the Maastrichtian, covering shallow marine to deep marine facies (Sundaram et al., 2001; Nagendra et al., 2011). Calcareous nannofossils are considered to be excellent for age dating Mesozoic (Jurassic and Cretaceous) marine sections, either independently, or in conjunction with ammonites and/or planktonic foraminifera. The potential of rich and abundant calcareous nannofossils, along with
macrofossils, has encouraged a detailed re-investigation of the exposed outcrops of the Karai
Formation (Fm.) in the Cauvery Basin. Here we present a new biostratigraphic study based upon
high-resolution nannofossil investigations and correlation of two sections, Karai and
Garudamangalam, that were sampled and collected during the same field session as Gale et al.
(2002) and Gale et al. (2019).

75

76 The goal of this study is to apply nannofossil biostratigraphy to the two sections 77 belonging to the Karai Fm. and to compare the results with previous investigations in the same 78 area. These two measured sections complement the relatively few sections that have been 79 previously analysed for biostratigraphy in the onshore Cauvery Basin and provide a platform for 80 testing the established nannofossil zonation schemes well away from the NW European and 81 Tethyan margin areas where they were originally developed. The Albian-Cenomanian and 82 Cenomanian-Turonian stage boundaries have been evaluated and compared in the two sections 83 using nannofossil proxies. Additionally, the composition of nannofossil assemblages were 84 assessed to better understand their palaeobiogeographic affinities.

85

86 2. Geological history and Cretaceous stratigraphy

87

The origin of the Cauvery Basin is linked to fragmentation of eastern Gondwanaland and was initiated by the rifting of India from Antarctica-Australia during the Late Jurassic to Early Cretaceous (Powell et al., 1988; Veevers et al., 1991). This rifting led to the subsequent development of the eastern segment of the Indian Ocean during the early part of the Cretaceous 92 (Holmes and Watkins, 1992). The Cauvery Basin became tectonically active following
93 downwarping of the eastern part of the Indian shield along a NE-SW basement trend, followed
94 by a series of extensional block-faulted movements along normal faults during the Cretaceous.
95 The Cenozoic witnessed continued basinal tilt towards the east, resulting in an easterly shift of
96 the depocentres (Sastri et al., 1981).

97

98 Initial non-marine syn-rift sedimentation (?Barremian-Aptian) in the basin was followed 99 by marine sedimentation during the post-rift, passive margin stage from the Albian onwards. 100 Multiple episodes of transgression, regression, deposition, and erosion are documented from the 101 Early Cretaceous to the Cenozoic, reflecting rift, pull-apart, sag, and tilt phases. The basin today 102 preserves a thick succession of well-exposed Lower Cretaceous to Holocene sedimentary rocks 103 (see reviews by Sastri et al., 1981; Prabhakar and Zutshi, 1993; Sundaram et al., 2001 and 104 Watkinson et al., 2007). Lithostratigraphy of the exposed onshore Cauvery Basin is established 105 with lateral and vertical facies variations relative to sea level changes, but as a result of several 106 workers contributing to the lithostratigraphy, there are conflicts in the nomenclature and 107 classification (e.g., Banerji, 1972; Sundaram & Rao, 1986; Acharyya & Lahiri, 1991; Kale and 108 Phansalkar 1992a; Tewari et al., 1996a; Sundaram et al., 2001; Ramkumar et al., 2004, 2011; 109 Nagendra & Nallapa Reddy, 2017). In this study, the lithostratigraphic division of Kale and 110 Phansalkar (1992a) and Paranjape et al. (2015) has been followed for the Uttatur Group/Karai 111 Fm. (Fig. 2).

112

113 The sections we studied are located within the Pondicherry Sub-basin, which is famous 114 for its Cretaceous outcrops. Sedimentary deposits in the sub-basin can be divided into the syn-

115 rift, continental sediments of the Sivaganga Fm., overlain unconformably by the post-rift, marine 116 sediments of the Uttatur, Trichinopoly, and Ariyalur groups respectively (Nagendra et al., 2011). 117 The Uttatur Group is sub-divided into the Karai and Dalmiapuram formations. The Karai Fm. 118 comprises the oldest marine strata in the basin and was dated as late Albian to middle Turonian 119 by Sundaram and Rao (1986). It is a mudstone dominated facies overlying the break-up 120 unconformity or onlapping onto Precambrian crystalline basement in the western extremities of 121 the basin (Paranjape et al., 2015). The upper contact of the Karai Fm. with the Trichinopoly 122 Group is marked by a middle Turonian hiatus (Paranjape et al., 2013). The formation is further 123 sub-divided into the Gypsiferous Clay and Sandy Clay Member, which comprise glauconitic, 124 gypsiferous clays with interbeds of sandy limestones and sandstones of variable grain sizes, and 125 rich in megafauna and microfossils (Ramkumar et al., 2004).

126

127 A GPlates palaeogeographic reconstruction (Fig. 3) for ~106 Ma (middle Albian) 128 suggests a palaeolatitude of ~45.75°S for the Cauvery Basin (Matthews et al., 2016). The 129 palaeobathymetry of the basin during Karai Fm. deposition is estimated to be outer neritic (100-130 200 m), based on benthic foraminifera and clay mineral analyses (Nagendra et al., 2013). 131 Previous work on foraminifera (e.g., Narayanan, 1977; Raju et al., 1991; Raju et al., 1993; Hart 132 et al., 2001; Venkatachalapathy and Ragothaman, 1995a, b; Venkatachalapathy et al., 2014) and 133 nannofossils (e.g., Kale and Phansalkar 1992a, b; Kale et al., 2000) of the Karai Fm. (Uttatur 134 Group) is generally of lower stratigraphic resolution compared to this study, but provides a 135 useful context within which the results of this study can be placed (see Discussion). 136

137 **3. Material and Methods**

139	Two complementary, overlapping stratigraphic sections, located approximately 5 km
140	apart, near the villages of Karai and Garudamangalam (Fig. 1), were selected for study in order
141	to provide a relatively complete lower Albian to lower Turonian succession. The sections
142	comprise marls and calcareous clays, weathering to brown and grey (black in subcrop, according
143	to Sundaram et al., 2001), and are variably glauconitic. Thin, glauconitic, strongly bioturbated
144	sandy beds, typically <10 cm in thickness are present, and possibly represent storm beds or
145	turbidites. Thicker sandstones contain moulds of aragonitic fossils. Pyrite nodules, including
146	steinkerns of molluscs, are abundant at certain levels, and calcareous, phosphatic, and barite
147	concretions occur less frequently. Belemnites, oysters, and serpulid worms are the most common
148	calcitic fossils.
149	
150	3.1. The Karai Section
151	
152	The Karai section (see Text-figs. 3–4 in Gale et al., 2019) is located in sparsely vegetated
1.50	
153	badlands, north of and parallel with the road from Karai to Kulakkalnattam. A 480 m succession
153 154	badlands, north of and parallel with the road from Karai to Kulakkalnattam. A 480 m succession was logged and sampled, on average every 4.5 m, through the section. Important
154	was logged and sampled, on average every 4.5 m, through the section. Important
154 155	was logged and sampled, on average every 4.5 m, through the section. Important lithostratigraphic markers include a highly glauconitic unit (9–13.5 m), a series of five fine silty
154 155 156	was logged and sampled, on average every 4.5 m, through the section. Important lithostratigraphic markers include a highly glauconitic unit (9–13.5 m), a series of five fine silty sandstones (198–211 m), and a disconformable surface, overlain by a shell bed, at 411 m, which

locality with palaeoenvironmental interpretation based on trace fossils was provided byParanjape et al. (2015).

162

163 3.2. The Garudamangalam Section

164 This section is exposed in badlands 2 km WNW of the village of Garudamangalam (see 165 Text-fig. 6 in Gale et al., 2019), and ~200 m of Karai Fm. was logged and sampled, on average 166 every 3 m, in a series of four traverses (A–D). The succession comprises calcareous clays and 167 marls, with frequent red and yellow coloured, bioturbated sandstone beds, 10–50 cm in 168 thickness. Pyritic molluscs are preserved at some levels. The lower part, up to 100 m, contains 169 common to abundant belemnites; at 107 m, oysters become common, and persist up to 150 m. 170 Important lithostratigraphic markers include three red sandstones, from 53–61 m, and a double 171 sandstone pair at 108-9 m.

172

173 3.3. Nannofossil observation

174

175 A total of 203 samples were collected for nannofossil study from the Karai (138 samples) 176 and Garudamangalam (65 samples) sections (Supplementary Material, Appendix A: Nannofossil 177 sample/slide list with curatorial designation, housed in the Department of Earth Sciences, 178 University College London). Calcareous nannofossils were analysed using simple smear slides 179 and standard light microscope (LM) techniques (Bown and Young, 1998). The volume of 180 sediment used for each smear slide preparation was standardised to ensure equal sample density. 181 A BH-2 Olympus transmitted light microscope was used to view nannofossils under cross-182 polarized and phase-contrast light. Nannofossils were analysed semi-quantitatively, with a

183	minimum of 500 fields of view (FOV) examined per sample via multiple (>20) traverses taken
184	vertically and horizontally across each slide.

186	Five categories were used to denote species abundances, defined as follows: Abundant
187	(A) - >10 specimens/FOV; Common (C) - 1–10 specimens/FOV; Frequent or Few (F) - 1
188	specimen/2–10 FOVs; Rare (R) - 1 specimen/>10 FOVs; Very Rare (VR) - 1 or 2 specimens in a
189	sample. An estimate of total calcareous nannofossil abundance in relation to inorganic
190	components in each sample was recorded per the following scale: High (H) - $\geq 20-30$
191	nannofossils/FOV; Moderate (M) - 3-10 nannofossils/FOV; Low (L) - <3 nannofossils/FOV;
192	and Barren (B) meaning no nannofossils were observed in a sample.
193	
194	The state of preservation, often ranging between two categories, was assessed for each
195	sample, according to the following criteria: G (good) - specimens show very little evidence of
196	overgrowth or etching and their identification is straightforward; M (moderate) - specimens
197	exhibit moderate effects of secondary alteration from etching and/or overgrowth, but
198	identification of species is not impaired; and P (poor) - specimens exhibit strong effects of
199	etching and/or overgrowth and identification may be difficult for some species.
200	
201	Nannofossil biostratigraphy is described based on first and last occurrences (FO and LO)
202	of identified marker species using the zonation scheme of Bown et al. (1998) and Burnett (1998).
203	The zonation schemes of Sissingh (1977), Perch Nielsen (1985), and Bralower et al. (1993,
204	1995) were also applied for comparison. The abbreviation NF is used for nannofossil while
205	describing the zones. FO is used for the first or stratigraphically lowest occurrence of the species

206	in the section. FCO refers to the first consistent occurrence of the species in the section and
207	typically occurs stratigraphically higher than the FO. LO is used for the last or stratigraphically
208	highest occurrence of the species in the section.
209	
210	4. Results
211	4.1. Nannofossil preservation, abundance, and diversity
212	
213	Both the Karai and Garudamangalam sections contain abundant and diverse calcareous
214	nannofossil assemblages (see full distribution charts;
215	https://data.mendeley.com/datasets/yzrmmrd2dj/draft?a=e99ad7d2-74de-4bb5-8e5a-
216	caba5ed84753). Nannofossil abundance and preservation are variable, but preservation is overall
217	good to moderate (G-M). Preservation in the Albian part of the section is better than the
218	Cenomanian. Out of the 203 samples analysed in the two sections, 9 samples were barren of
219	nannofossils, but the rest yielded rich assemblages. The average species richness is comparable
220	in the two sections: 54 species at Karai and 50 species in Garudamangalam. A total of \sim 155 taxa
221	were identified (Supplementary Material, Appendix B: taxonomic list) with many species being
222	reported for the first time from the Cauvery Basin in this study. Four new species Calculites
223	karaiensis, Loxolithus bicyclus, Manivitella fibrosa, and Tranolithus simplex are described
224	herein (see Systematic Palaeontology and Figs. 4-8).
225	
226	4.2. Biostratigraphy

228	The FO and LO of index species in the study sections were used to identify the BC zones
229	of Bown et al. (1998) and the UC zones of Burnett (1998). Tables 1 and 2 list the important
230	nannofossil zonal and subzonal markers recognised in the Karai and Garudamangalam Section in
231	stratigraphic order. Biozones identified in this study are described below in stratigraphic order
232	from older to younger.
233	
234	Prediscosphaera columnata Zone (BC23) Aptian-Albian boundary interval to middle Albian.
235	Defined by the FO of Prediscosphaera columnata. Recognised in the lower Karai Section (22.5
236	m; sample KA0-KA22.5), where both P. columnata (subcircular) and small P. cf. P. spinosa
237	(subelliptical) are present. The FOs of C. hayi and H. albiensis are additional events recognised
238	in this zone.
239	
240	Tranolithus orionatus Zone (BC24) middle Albian. Defined by the FO of Tranolithus
241	orionatus. Recognised in the lower Karai Section (31.5 m; sample KA22.5-KA54).
242	
243	Axopodorhabdus albianus Zone (BC25) middle to upper Albian. Defined by the FO of
244	Axopodorhabdus albianus. Placed in the Karai Section at the FCO of A. albianus (sample KA54)
245	due to its inconsistent and rare occurrence in the lower samples KA22.5 and KA45. The use of
246	the FCO was proposed by Bown (2001) because A. albianus is inconsistent and rare at the base
247	of its range. The total thickness of the BC25 Zone is measured as 121.5 m (sample KA54-
248	KA175.5), but it could not be sub-divided into the Subzone BC25a and BC25b due to the
249	absence of Ceratolithina bicornuta. The FOs of C. anglicum and G. praeobliquum lie within this
250	zone.

252	Eiffellithus monechiae Zone (BC26) upper Albian. Defined by the FO of Eiffellithus
253	monechiae. Recognised in the Karai Section (~9 m; sample KA175.5–KA184.5). The FO of B.
254	enormis is recorded in this zone.
255	
256	Eiffellithus turriseiffelii Zone (BC27a-c/UC0a-c) upper Albian to lower Cenomanian. Defined
257	by the FO of Eiffellithus turriseiffelii. Recognised in full at Karai, but partially at
258	Garudamangalam, as <i>E. turriseiffellii</i> is already present in the lowermost sample. The thickness
259	of the zone is 116.5 m at Karai (sample KA184.5–KA301) and 96.5 m (sample GM0–GM96.5)
260	at Garudamangalam. Subzone BC27a is recognised in both sections, based on the LO of
261	Hayesites albiensis. However, Subzone BC27b-c, could not be distinguished because Calculites
262	anfractus is practically absent in both sections (questionable occurrence in a single sample in
263	Garudamangalam). The FOs of C. ehrenbergii and G. theta, and the LO of C. anglicum are
264	recorded in the BC27a Subzone in the Karai section. The FOs of <i>B. enormis</i> , <i>G. chiasta</i> , <i>G.</i>
265	ponticula, G. segmentatum, G. theta, and the LOs of G. chiasta, G. stenostaurion, G. theta, and
266	W. britannica are found within the combined BC27b-c Subzone in the Garudamangalam section.
267	
268	UC1 NF Zone lower Cenomanian. Defined by the FO of Corollithion kennedyi, this zone is
269	103.5 m thick at Karai (sample KA301-KA404.5) and 16.5 m thick at Garudamangalam (sample
270	GM96.5–GM113). Subzones a to d were not identified because the subzonal markers were not
271	identified in the stratigraphic order described in Burnett (1998). Some of the defining events,
272	e.g., LO of G. chiasta, LO of W. britannica, are found stratigraphically lower, or higher, with

273	reference to the FO of C. kennedyi, and their order is variable in the two sections. Other
274	secondary events, e.g., FO of H. anceps, are absent.

276 UC2 NF Zone lower to basal middle Cenomanian. Defined by the FO of Gartnerago 277 segmentatum. This zone is not differentiated at Karai because of the simultaneous FOs of G. 278 segmentatum and L. acutus in the sample KA404.5. The zone is not recognised at 279 Garudamangalam because the FO of G. segmentatum occurs stratigraphically lower than the FO 280 of C. kennedyi in the upper Albian to lower Cenomanian BC27b-c Subzone interval. 281 282 **UC3 NF Zone** middle to upper Cenomanian. Defined by the FO of *Lithraphidites acutus*, this 283 zone is 44.4 m thick at Karai (sample KA404.5–KA448.9) and 70.5 m thick at Garudamangalam 284 (sample GM113–GM183.5). In both sections, the UC3 Zone was sub-divided into a combined 285 UC3a-b (LO of S. gausorhethium) and UC3c-d (LO of C. kennedyi), but subzones UC3b (LO of 286 G. theta) and UC3d (LO of G. nanum) could not be differentiated individually because the index 287 taxa were either not present in the expected stratigraphic order, e.g., G. theta, which was found 288 stratigraphically lower than L. acutus, or were absent (G. nanum). Additional events recognised 289 in the UC3a-b interval include the FOs of C. sculptus and M. belgicus, and the LOs of G. 290 ponticula and S. gausorhethium. Secondary events falling within the UC3c-d interval include the 291 FO of *M. decoratus*, and the LOs of *C. striatus* and *C. kennedyi*. The FO of *Ahmuellerella* cf. *A.* 292 octoradiata occurs in the UC3a-b interval at Karai, but occurs higher, in the UC3e Subzone at 293 Garudamangalam.

UC4 NF Zone upper Cenomanian. Defined by the FO of *Cylindralithus biarcus* but not
 differentiated because this index species is missing.

297

UC5 NF Zone upper Cenomanian to lower Turonian. Defined by the LO of *Lithraphidites acutus*. The zone is interpreted as not present, as the LOs of *L. acutus* and *H. chiastia* occur in
the same sample in both sections. This suggests the presence of a hiatus, equivalent to Zone
UC5.

302

303 UC6 NF Zone lower Turonian. Defined by the LO of Helenea chiastia, the zone is present in the 304 Karai Section with a thickness of 20.2 m (sample KA448.9-KA469.1). The lower boundary of 305 the zone occurs at a hiatus (see above). Subzones UC6a and UC6b are distinguished based on the 306 FO of *Eprolithus moratus*. The FO of *E. octopetalus* is recorded in the UC6a Subzone at Karai. 307 UC6 Zone cannot be applied to the Garudamangalam Section, as no lower Turonian markers 308 (e.g., E. moratus, E. octopetalus, Quadrum gartneri) were identified in the samples. The highest 309 Karai sample (KA469.1) falls within the UC6b Subzone. Q. gartneri is not observed in any of 310 the samples.

311

Nannofossil biostratigraphy shows that the lower to upper Albian NF Zones BC23
through BC27 of Bown et al. (1998) are present in the Karai Section, with the upper Albian Zone
BC27 being the lowest recognised in the Garudamangalam Section. The Albian zones are
divisible into subzones for the most part, with some exceptions (e.g., BC25a/ BC25b Subzone).
In the Cenomanian, the UC zones of Burnett (1998) were applied, but only Zone UC1 (FO of *C. kennedyi*) and UC3 (FO of *L. acutus*) could be recognised with confidence. The UC2 (FO of *G.*

318	segmentatum) and UC4 Zone (FO of C. biarcus) could not be differentiated. Zone UC5 is not
319	identified because of the presence of a hiatus. Several Cenomanian zonal and subzonal marker
320	species are either not present, e.g., FO of C. anfractus (within UC0), FO of H. anceps (within
321	UC1), LO of <i>I. compactus</i> (within UC3d), FO of <i>C. biarcus</i> (UC4), LO of <i>L. acutus</i> (UC5); or
322	not consistent with the stratigraphic order reported in Burnett (1998), e.g., LO of W. britannica
323	(UC1b), FO of G. segmentatum (UC2), thus preventing their use here. However, it is worth
324	mentioning that Cenomanian zonal markers from the earlier CC (Sissingh, 1977; Perch-Nielsen,
325	1985) and NC zonation schemes (Roth, 1978; Bralower et al., 1993; 1995) such as C. kennedyi,
326	M. decoratus, L. acutus, and H. chiastia, are all present. This suggests that the applicability of
327	some of these more recently proposed bioevents may be problematic rather than there being
328	significantly missing stratigraphy.
329	
330	4.3. Systematic palaeontology
331	
332	This section provides LM images of a representative selection of nannofossil taxa from
333	the Karai Fm. (Figs. 4-8). The LM images are reproduced at constant magnification with a 2µm

334 scale bar shown in the top left corner. Taxonomic description of four new species, *Calculites*

335 karaiensis, Loxolithus bicyclus, Manivitella fibrosa and Tranolithus simplex, are included herein.

The taxonomy follows the scheme of Bown & Young (1997) and the online nannoplankton

337 database, Nannotax (Young et al., 2017; http://www.mikrotax.org/Nannotax3). The descriptive

terminology follows the guidelines of Young et al. (1997). Only those bibliographic references

that are not included in Perch-Nielsen (1985) and Nannotax are given in the references.

341 342	HETEROCOCCOLITHS		
343 344	Murolith coccoliths		
345	Family Chiastozygaceae Rood et al., 1973 emend. Varol & Girgis, 1994		
346	Genus Loxolithus Noël, 1965		
347 348	Type species: Cyclolithus armilla Black, in Black & Barnes, 1959		
349	Loxolithus bicyclus sp. nov.		
350	Fig. 4, no. 9–12		
351	1998 <i>Loxolithus</i> sp. 2, Bralower and Bergen, p. 75, pl. 1, fig. 2		
352	Derivation of name: From 'cyclus' in Latin meaning cycle, referring to the two distinct rim		
353	cycles observed in the species. Diagnosis: Medium to large-sized elliptical muroliths with a		
354	narrow bicyclic rim and a broad, open, central area. The inner rim cycle is bright in XPL with		
355	spiralling extinction lines. Differentiation : The species is distinguished from <i>L. armilla</i> by its		
356	clearly bicyclic rim, whereas L. armilla is unicyclic. Holotype: Fig. 4, no. 9. Paratype: Fig. 4,		
357	no. 11 (11 and 12 are the same specimen). Dimensions : Holotype L = 8.5 μ m; Paratype L =		
358	6.75 μm. Type locality: Garudamangalam, Cauvery Basin, India. Type level: Karai Fm., lower		
359	Cenomanian, sample GM101, Zones UC1. Abundance: Rare. Occurrence: Zone BC27–UC6		
360	(upper Albian–lower Turonian), Karai Fm.		
361 362	Genus Tranolithus Stover, 1966		
363	Type species: Tranolithus manifestus Stover, 1966		
364	Tranolithus simplex sp. nov.		
365	Fig. 4, no. 27–32		
366			

367	Derivation of name: From 'simplex' in Latin meaning simple, referring to the simple
368	appearance of the central area transverse bar. Diagnosis: A small to medium-sized murolith with
369	a narrow rim and broad central area spanned by a simple transverse bar. Description: The
370	narrow rim appears unicyclic in XPL, and the rim and bar have similar, low birefringence, with
371	the bar being slightly brighter. A central hole in the bar is most likely a spine base.
372	Differentiation: Similar to the Jurassic species Zeugrhabdotus erectus but the latter has a more
373	birefringent bar which is clearly crystallographically disjunct. Remarks: The species has been
374	placed within the genus Tranolithus and not Zeugrhabdotus because the overall LM appearance
375	is closer to other Tranolithus species such as T. orionatus and T. gabalus, however the
376	distinction between these two genera is questionable. Holotype: Fig. 4, no. 27. Paratype: Fig 4,
377	no. 30 (30–32 are the same specimen). Dimensions: Holotype $L = 7.5 \ \mu m$; Paratype $L = 8.0$
378	µm. Type locality: Karai, Cauvery Basin, India. Type level: Karai Fm, lower Cenomanian;
379	sample KA373 (Subzone UC1). Abundance: Frequent to Rare. Occurrence: Zone BC23–UC6
380	(lower Albian–lower Turonian), Karai Fm.
381	
382 383	Placolith Coccoliths
384	Family Tubodiscaceae Bown & Rutledge in Bown & Young, 1997
385	Genus Manivitella Thierstein, 1971
386	Type species: Cricolithus pemmatoideus Deflandre in Manivit, 1965 designated by Thierstein,
387	1971
388	Manivitella fibrosa sp. nov.
389	Fig. 7, no. 1–6
390	

391	Derivation of name: From 'fibra' in Latin meaning fibre, referring to the fibrous, striated
392	appearance of the coccolith rim. Diagnosis: Large, elliptical placolith with a narrow, striated rim
393	and a broad, vacant central area. The rim is composed of two narrow shields that are dark in XPL
394	and a third, very narrow and rather high collar-cycle which is bright in XPL. The distal shield
395	has a highly striated appearance in XPL. Under PC, the rim appears as a dark band of uniform
396	thickness. Differentiation: In XPL this species is darker than M. pemmatoidea and the distal
397	shield is more finely striated. The outer edge of the inner cycle is not beaded in appearance,
398	which makes the separation easier from <i>M. pemmatoidea</i> . This species does not have a clearly
399	bicyclic appearance (in XPL) that is characteristic of the genus Tubodiscus (e.g., T. burnettiae),
400	hence it is placed under the genus Manivitella. Holotype: Fig. 7, no. 2. Paratype: Fig. 7, no. 4.
401	Dimensions: Holotype $L = 13.5 \ \mu m$; Paratype $L = 14.5 \ \mu m$. Type locality: Karai, Cauvery
402	Basin, India. Type level: Karai Fm, upper Albian, sample KA278.5 (Zone BC27). Abundance:
403	Frequent to Rare. Occurrence: Zone BC24–UC3 (middle Albian–middle Cenomanian), Karai
404	Fm.
405	
406	HOLOCOCCOLITHS
407	Family Calyptrosphaeraceae Boudreaux & Hay, 1969
408	Genus Calculites Prins & Sissingh in Sissingh, 1977
409	Type species: Tetralithus obscurus Deflandre, 1959
410	
411	Calculites karaiensis sp. nov.
412	Fig. 7, no. 40–42; Fig. 8, no. 1–8
413	

414 Derivation of name: From 'Karai', the place from which it is described. Diagnosis: An elliptical, small holococcolith with a rim formed from 6 to 7 blocks. The blocks are 415 416 crystallographically distinct, asymmetric, and separated by slightly irregular sutures. A 417 longitudinal and two diagonal sutures can usually be distinguished. The surface of the 418 holococcolith appears to be smooth under LM. Differentiation: Distinguished from other mid-419 Cretaceous holococcolith species, which typically have 4 or less blocks, by the possession of 6–7 420 irregular blocks (compare with C. percernis, Fig. 7, no. 38-39). Holotype: Fig. 8, no.1. **Paratype**: Fig. 8, no. 6 (6–8 are the same specimen). **Dimensions**: Holotype $L = 4.5 \mu m$; 421 422 **Paratype** $L = 6.0 \mu m$. Type locality: Karai, Cauvery Basin, India. Type level: Karai Fm., lower 423 Turonian, sample KA459.3 (Subzone UC6b). Abundance: Frequent, observed in two samples 424 (KA445.7, KA459.3). Occurrence: Subzone UC3c-d–UC6b (middle Cenomanian–lower 425 Turonian), Karai Fm.

407	_	D' '
427	`	Discussion
121	U •	Discussion

428 429 430 431	5.1. Stratigraphic remarks
432	5.1.1. Albian zonation
433 434	The Albian marker species P. columnata, T. orionatus, A. albianus, E. monechiae, and E.
435	turriseiffelii are all readily recognised in the Karai Section demonstrating the cosmopolitan
436	nature of these biostratigraphically useful taxa. P. columnata is present in the lowest sample
437	examined (KA0), indicating an intra-BC23 NF Zone (or CC8a Subzone) position for the base of
438	the Karai Section. The FO of P. columnata (subcircular) occurs in the very uppermost Aptian in

the Albian GSSP (Kennedy et al., 2000; 2014) and so provides a good approximation for thisstage boundary.

442	The BC25a/ BC25b (LO of C. bicornuta) and BC27c (FO of C. anfractus) NF subzones
443	could not be differentiated in this study, due to the absence of the index species. Several other
444	secondary markers used in the BC zonation, such as C. hamata, B. boletiformis, and T.
445	tessellatus are also absent in the Karai Fm. All of these taxa are thought to be restricted to NW
446	European high-latitudes (Crux, 1991; Bown, 2001), making their absence in the Cauvery Basin
447	notable, but not entirely surprising.
448	
449	A noteworthy feature of the Karai nannoflora is the early stratigraphic appearance of
450	Crucibiscutum hayi in the lower Albian (sample KA4.5, BC23 Zone), contrasting with its
451	reported first appearance in the BC27 NF Zone (or CC9b Subzone) in the upper Albian (Bown,
452	2001). Based on this observation, an Austral (southern high-latitude) origin during the early
453	Albian is proposed for this species, along with a subsequent migration to Tethyan and Boreal
454	latitudes during the late Albian.
455 456 457 458 459 460	5.1.2. <i>Cenomanian and Turonian zonation</i> The UC zonation scheme of Burnett (1998) was developed in order to improve Upper
461	Cretaceous biostratigraphic resolution by replacing problematic markers from the earlier CC and
462	NC zonation schemes of Sissingh (1977) and Roth (1978). Biogeographic differences are
463	accommodated through the provision of separate information for two regions, Europe and the
464	Indian Ocean, with the Indian Ocean region sub-divided into the Tethyan-Intermediate and

465 Austral provinces. In this study, the global suite of UC zones and subzones, irrespective of
466 region or province, was taken into consideration to test its applicability and obtain the best
467 stratigraphic resolution for the studied sections.

468

469 The Cenomanian to lower Turonian UC zones and subzones are not uniformly applicable 470 in the two sections due to rarity of the index species, inconsistent stratigraphic ordering 471 compared with Burnett (1998), or stratigraphic breaks in the section (Figure 9a, b). Calculites 472 anfractus was practically not identified in the Cauvery Basin, preventing the identification of 473 Subzone BC27c/UC0c, but the rarity or absence of this species has been noted elsewhere (Gale 474 et al., 2011), suggesting that the subzone is probably not globally applicable. The subzonal 475 bioevents FO of H. anceps (UC1 Zone; Europe/ Indian Ocean), FO of O. intermedium (UC5 476 Zone; Europe/ Indian Ocean), LO of I. compactus (UC3 Zone; Europe), LO of R. hollandicus 477 (UC1 Zone, Europe/ Indian Ocean) were also not identified in the Karai sections, but again these 478 events do not appear to be consistently reported. Other subzonal markers are present, but they 479 could not be used to assign subzones either because of rare occurrence (e.g., FO of C. sculptus, 480 FO of L. pseudoquadratus), or inconsistencies in their relative stratigraphic order (e.g., LO of W. 481 britannica, FO of P. cretacea) with respect to zone defining datums (e.g., FO of C. kennedyi) in 482 the two sections. Table 3 gives a summary of the Cenomanian zone and subzone markers used in 483 Burnett (1998) and Lees (2002) compared with the Cauvery Basin.

484

The FO of *G. segmentatum* varies in its stratigraphic positioning in the two sections. At
Karai, the FCO of *G. segmentatum* coincides with the FO of *L. acutus*, rendering the UC2 Zone

- 487 inapplicable in the section. At Garudamangalam, the FCO of G. segmentatum lies
- 488 stratigraphically lower (Subzone BC27b–c) than the FO of *C. kennedyi* (UC1 Zone). As a result,

489	the UC2 Zone is not recognized in this section either, however, we consider this is likely due to
490	an extended lower range for G. segmentatum, rather than any significant stratigraphic hiatus (see
491	further discussion below). Distinct size shifts are seen in G. segmentatum with early forms,
492	referred to here as G. cf. G. segmentatum, being relatively small (~5 µm in length) and larger,
493	more typical sizes (> 8 μ m in length) and more consistent occurrences found stratigraphically
494	higher, after a gap of ~45–75 m (FCO, samples KA404.5 and GM62). Small sizes are rarely
495	observed after the FCO of the species. The early appearance of this species in the late Albian at
496	Garudamangalam suggests that G. segmentatum may have evolved earlier in southern high-
497	latitudes, before migrating to Boreal regions, comparable to the observation made for C. hayi in
498	the early Albian. In general, Gartnerago is considered a high-latitude form, and may be
499	particularly common in the Austral area (Thierstein, 1981; Lees, 2002).
500	
501	Cylindralithus biarcus (= Rotelapillus biarcus of Lees and Bown, 2005) is questionably
• • -	
502	identified in the Cenomanian at Karai (sample KA435.9, UC3 Zone) but not at
502	identified in the Cenomanian at Karai (sample KA435.9, UC3 Zone) but not at
502 503	identified in the Cenomanian at Karai (sample KA435.9, UC3 Zone) but not at Garudamangalam. Very rare specimens were found in two samples in the Turonian section
502 503 504	identified in the Cenomanian at Karai (sample KA435.9, UC3 Zone) but not at Garudamangalam. Very rare specimens were found in two samples in the Turonian section (KA469.1, KA464.2). Overall, the FO of this species could not be reliably identified. As a result,
502 503 504 505	identified in the Cenomanian at Karai (sample KA435.9, UC3 Zone) but not at Garudamangalam. Very rare specimens were found in two samples in the Turonian section (KA469.1, KA464.2). Overall, the FO of this species could not be reliably identified. As a result, the Zone UC4 could not be differentiated, but we consider this is due to the unreliability of the
502 503 504 505 506	identified in the Cenomanian at Karai (sample KA435.9, UC3 Zone) but not at Garudamangalam. Very rare specimens were found in two samples in the Turonian section (KA469.1, KA464.2). Overall, the FO of this species could not be reliably identified. As a result, the Zone UC4 could not be differentiated, but we consider this is due to the unreliability of the
502 503 504 505 506 507	identified in the Cenomanian at Karai (sample KA435.9, UC3 Zone) but not at Garudamangalam. Very rare specimens were found in two samples in the Turonian section (KA469.1, KA464.2). Overall, the FO of this species could not be reliably identified. As a result, the Zone UC4 could not be differentiated, but we consider this is due to the unreliability of the index species, rather than the presence of any significant stratigraphic gap.
502 503 504 505 506 507 508	identified in the Cenomanian at Karai (sample KA435.9, UC3 Zone) but not at Garudamangalam. Very rare specimens were found in two samples in the Turonian section (KA469.1, KA464.2). Overall, the FO of this species could not be reliably identified. As a result, the Zone UC4 could not be differentiated, but we consider this is due to the unreliability of the index species, rather than the presence of any significant stratigraphic gap. In the uppermost Cenomanian part of the Karai Section, the co-occurring LOs of several

(GM183), but the LO of *A. albianus* is recorded slightly lower in the section (GM170.5). The LO of *H. chiastia* defines the base of the UC6 Zone, and the latter is considered a reliable proxy for the Cenomanian-Turonian boundary (Burnett, 1998). Nannofossil data, therefore, suggests an apparent hiatus in the upper Cenomanian (UC5 NF Zone interval) at Garudamangalam as well, which falls within the *Calycoceras (C.) asiaticum* Ammonite Zone (Gale et al., 2019).

517

518 The lower Turonian is recognized at Karai, based on the presence of Eprolithus 519 octopetalus and E. moratus. The FO of E. moratus is used to define the Subzone UC6b. No 520 Turonian markers are present at the Garudamangalam Section, but the absence of *Eprolithus* 521 moratus in the samples above (GM183.5–GM191) the LO of *H. chiastia* (sample GM183) is 522 indicative of Subzone UC6a and the lower Turonian. This, however, conflicts with the ammonite 523 data (Gale et al., 2019), which indicates that the highest sediments present at Garudamangalam 524 fall within the upper Cenomanian Pseudocalycoceras (P.) harpax Ammonite Zone, 525 Euomphaloceras (E.) euomphalum fauna. This fauna indicates a position low within the upper 526 Cenomanian (Fig. 9b).

527

The nannofossil marker, *Zeugrhabdotus xenotus*, is reworked in the upper Cenomanian and lower Turonian section at Garudamangalam (samples GM174 and GM190), which is the only obvious example of reworking observed in the study. *Quadrum gartneri* is not observed in any sample, even though it has been previously reported from the Uttatur Group (Kale and Phansalkar, 1992a; b). The identification of this taxon, and therefore the base of NF Zone UC7 in the lower Turonian is often problematic, most likely due to its rare and sporadic distribution (Berrocoso et al., 2012, etc.).

536	The stratigraphic thickness of the identified nannofossil zones varies between the two
537	sections, with the majority of zones thicker at Karai (total thickness, ~480 m) compared with
538	Garudamangalam (total thickness, ~200 m). The exception is the middle–upper Cenomanian
539	UC3 NF Zone, which is thicker in Garudamangalam (~70 m) than Karai (~45 m). This can be
540	attributed to local variations in basin sedimentation rates (Figure 10 a, b; age-depth plots). Kale
541	and Phansalkar (1992b) have reported a condensed middle Cenomanian section (CC10, M.
542	decoratus Zone) in the Terani-Garudamangalam section of the Cauvery Basin on the basis of
543	nannofossil data, but not in the Karai-Kulakkalnattam section.
544	
545	5.2. Albian-Cenomanian and Cenomanian-Turonian stage boundary
546	
547	The Albian-Cenomanian boundary appears to be stratigraphically continuous in
547 548	The Albian-Cenomanian boundary appears to be stratigraphically continuous in the studied sections, at least at the level of biostratigraphic resolution achieved in this study, with
548	the studied sections, at least at the level of biostratigraphic resolution achieved in this study, with
548 549	the studied sections, at least at the level of biostratigraphic resolution achieved in this study, with the base of the Cenomanian identified at Karai a short distance beneath the sample KA341.5
548 549 550	the studied sections, at least at the level of biostratigraphic resolution achieved in this study, with the base of the Cenomanian identified at Karai a short distance beneath the sample KA341.5 (341.5 m), and at Garudamangalam close to the sample GM53 (53 m), using the FO of lower
548 549 550 551	the studied sections, at least at the level of biostratigraphic resolution achieved in this study, with the base of the Cenomanian identified at Karai a short distance beneath the sample KA341.5 (341.5 m), and at Garudamangalam close to the sample GM53 (53 m), using the FO of lower Cenomanian ammonites of the <i>M. mantelli</i> Ammonite Zone. The first occurrence of lower
548 549 550 551 552	the studied sections, at least at the level of biostratigraphic resolution achieved in this study, with the base of the Cenomanian identified at Karai a short distance beneath the sample KA341.5 (341.5 m), and at Garudamangalam close to the sample GM53 (53 m), using the FO of lower Cenomanian ammonites of the <i>M. mantelli</i> Ammonite Zone. The first occurrence of lower Cenomanian ammonites appears to be more consistent in the studied sections than the FO of <i>C</i> .
 548 549 550 551 552 553 	the studied sections, at least at the level of biostratigraphic resolution achieved in this study, with the base of the Cenomanian identified at Karai a short distance beneath the sample KA341.5 (341.5 m), and at Garudamangalam close to the sample GM53 (53 m), using the FO of lower Cenomanian ammonites of the <i>M. mantelli</i> Ammonite Zone. The first occurrence of lower Cenomanian ammonites appears to be more consistent in the studied sections than the FO of <i>C.</i> <i>kennedyi</i> to delineate the base of the Cenomanian (see Discussion in Section 5.4). Recent studies
 548 549 550 551 552 553 554 	the studied sections, at least at the level of biostratigraphic resolution achieved in this study, with the base of the Cenomanian identified at Karai a short distance beneath the sample KA341.5 (341.5 m), and at Garudamangalam close to the sample GM53 (53 m), using the FO of lower Cenomanian ammonites of the <i>M. mantelli</i> Ammonite Zone. The first occurrence of lower Cenomanian ammonites appears to be more consistent in the studied sections than the FO of <i>C.</i> <i>kennedyi</i> to delineate the base of the Cenomanian (see Discussion in Section 5.4). Recent studies support the observation regarding the anomalous FO of <i>C. kennedyi</i> (Silva Jr. et al., 2020). At the

558	Table 4 provides a comparison of the nannofossil bioevents around the Albian-
559	Cenomanian boundary in the Mont Risou section (Burnett in Gale et al., 1996) and the Cauvery
560	Basin. Most nannofossil bioevents are common to both regions, although there are some
561	inconsistencies in the relative stratigraphic order of the events. The FOs of G. chiasta, G. theta,
562	and <i>G. ponticula</i> , and the LOs of <i>E. paragogus</i> (= <i>S. glaber</i>), <i>H. albiensis</i> , and <i>W. britannica</i> all
563	support identification of the boundary interval in the Cauvery Basin. Kennedy et al. (2004)
564	reported the LO of Gartnerago stenostaurion (= Arkhangelskiella antecessor) in the upper
565	Albian at Mont Risou. G. stenostaurion shows a patchy distribution in the Cauvery sections and
566	was not used to evaluate the boundary in this study.

568 The Cenomanian-Turonian boundary is associated with a stratigraphic break (hiatus) in 569 both Cauvery sections. At Karai, the hiatus occurs between samples KA448.2 (448.2 m) and 570 KA448.9 (448.9 m), and is indicated by the co-occurring LOs of the upper Cenomanian index 571 species A. albianus, H. chiastia, and L. acutus, followed by the FO of the lower Turonian index 572 species, E. octopetalus. This is in agreement with ammonite and inoceramid occurrences (Fig. 573 9a; Gale et al., 2019). Biostratigraphically, the Cenomanian-Turonian boundary interval is 574 incomplete and Zone UC5 is missing. Zone UC4 was not differentiated due to the problematic 575 index species, C. biarcus. A comparable Cenomanian-Turonian boundary interval hiatus is 576 interpreted in Garudamangalam, even though the lower Turonian is inferred, based on the 577 absence of E. moratus in the samples above the LO of H. chiastia. However, this falls within the 578 upper Cenomanian Calycoceras asiaticum fauna (P. harpax Ammonite Zone; Gale et al., 2019), 579 demonstrating disparity here between nannofossil and ammonite biostratigraphies (Fig. 9b). This 580 study is the first to report an upper Cenomanian-lowermost Turonian unconformity in the Karai

581	Fm. on the basis of nannofossil data. At Karai, the duration of the hiatus is estimated to be ~ 0.66
582	Myr, using the calibrated ages for the LO of L. acutus (94.39 Ma) and the FO of E. moratus
583	(93.73 Ma) (Ogg and Hinnov, 2012). The magnitude of the hiatus is difficult to estimate at
584	Garudamangalam because of the lack of Turonian index species, but is likely similar to that
585	observed at Karai (Fig. 10b). Previously, Ramkumar et al. (2011) interpreted the Cenomanian-
586	Turonian boundary as an unconformity, marking a major sequence boundary in the Cauvery
587	Basin, using bulk geochemical profiles. Cenomanian-Turonian boundary hiatuses have also been
588	recognized elsewhere in the Indian Ocean (e.g., Kale and Phansalkar, 1992b; Lees, 2002).
589	Additionally, the stratigraphic order of extinctions of upper Cenomanian nannofossil indices,
590	such as A. albianus, C. kennedyi, and L. acutus, has been found to be inconsistent in outcrop and
591	core samples in the Cretaceous Western Interior Basin, USA (Bralower and Bergen, 1998;
592	Corbett and Watkins, 2013).
593	
594	5.3. Comparison with previous age interpretations (nannofossils and planktonic foraminifera)
595	
596	Previous nannofossil biostratigraphy of the Uttatur Group has been based on the same
597	outcrop and quarry samples documented in four publications (Jafar and Rai, 1989; Kale and
598	Phansalkar, 1992a; b; Kale et al., 2000). Five CC NF zones (Perch-Nielsen, 1979; 1985) were
599	recognised (Zone CC7-CC11) based on the FOs of C. litterarius, P. columnata, E. turriseiffelii,
600	M. decoratus, and Q. gartneri (Fig. 2). This succession of zones was described as continuous
601	without any stratigraphic breaks. In comparison, this study ascribes the age of the marine Karai
602	Section as ranging from the early Albian (BC23 Zone = CC8 Zone) to early Turonian (UC6b

Subzone = intra CC10 Zone), showing that the CC11 Zone (middle Turonian) identified in the
previous work, is not present.

606	Several papers describe foraminifera from the Karai Shale, but they are difficult to
607	correlate with this study because they are either based on wells/shallow cores (e.g., Govindan et
608	al., 1996; Tewari et al., 1996b) or outcrops, with very little stratigraphic and sample information
609	(Nagendra et al., 2013; Venkatachalapathy et al., 2014). Nagendra et al. (2013) interpreted the
610	age of the exposed Karai Shale in the badlands area as late Albian to middle Turonian, based on
611	the planktonic foraminifera index species Planomalina buxtorfi, Hedbergella portsdownensis,
612	Rotalipora reicheli, and Praeglobotruncana stephani. Details of the zones or species
613	distributions are not given in the paper, but overall, it can be said that although the planktonic
614	foraminiferal ages and the nannoplankton ages described in this study overlap to a degree, the
615	sections studied appear to have different locations with varying sampling resolutions.
616	
617	5.4. Comparison with ammonite stratigraphy
618	
619	In the Karai Section, upper Albian ammonites of the P. (S.) rostrata Zone first occur at
620	63 m, which falls within NF Zone BC25 (Figure 9a). This is a mismatch, because elsewhere, the
621	lower part of BC25 NF Zone falls within the middle Albian in terms of ammonite faunas. In the
622	Col de Palluel sections, southeastern France (Bown in Gale et al., 2011), the base of NF Zone
623	BC25 (FO of <i>A. albianus</i>) falls at or within the base of the middle Albian. The FO of <i>E.</i>
624	
021	turriseiffellii at 184.5 m, and the LO of H. albiensis at 278.5 m at Karai correspond in order to
625	<i>turriseiffellii</i> at 184.5 m, and the LO of <i>H. albiensis</i> at 278.5 m at Karai correspond in order to the FO and LO of these species in SE France, but there, <i>E. turriseiffellii</i> appears at the base of the

626	M. fallax Ammonite Zone, and H. albiensis within the D. perinflatum Ammonite Zone (Gale et
627	al., 2011; Fig. 49). At Karai, both appear within the P. (S.) rostrata Ammonite Zone.
628 629	At Karai, the FO of <i>C. kennedyi</i> at 301 m (base of NF Zone UC1) significantly predates
630	the FO of lower Cenomanian ammonites of the M. mantelli Zone at 341.5 m, whereas at
631	Garudamangalam, C. kennedyi appears at 96.5 m, above the occurrence of lower Cenomanian
632	ammonites, in a barren interval beneath the lowest middle Cenomanian ammonites of the C .
633	asiaticum Zone (Fig. 9b). In the UK and elsewhere (Burnett, 1998; see also Gale et al., 1996;
634	2011), C. kennedyi appears in the lowest subzone of the M. mantelli Ammonite Zone, the N.
635	carcitanense Ammonite Subzone.
636 637 638	At Karai, the base of NF Zone UC3 (FO of <i>L. acutus</i> , 404.5 m) falls in the uppermost part
639	of the lower Cenomanian, probably of M. dixoni Ammonite Zone age, immediately underlying
640	the FO of middle Cenomanian ammonites of the C. cunningtoni Ammonite Zone at 410 m. At
641	Garudamangalam, the base of UC3 NF Zone falls at 113 m, within the middle Cenomanian, and
642	close to the base of the C. asiaticum Ammonite Zone. In the UK, the base of NF Zone UC3 is
643	close to the base of the middle Cenomanian.
644 645	The absence of NF Zone UC5 at Karai, at a level of 448.9 m, marking a hiatus, is
646	matched by the absence of late Cenomanian ammonites of the <i>M. geslinianum</i> and <i>N. juddii</i>
647	Ammonite Zones, with which NF Zones UC4-5 correspond (Burnett, 1998). The association of
648	the lower Turonian inoceramid, Mytiloides, with nannofossils of Zone UC6 in the Karai Section
649	corresponds well with the occurrences in the UK (Burnett, 1998).
650	

651	Some of the mismatches between ammonite and nannofossil occurrences can perhaps be
652	related to non-preservation of ammonites at key intervals. For example, at Karai, there is a gap in
653	the ammonite record of 54 m between the LO of Albian mortoniceratids and the FO of lower
654	Cenomanian ammonites of the <i>M. mantelli</i> Zone, within which the base of NF Zone UC1 (FO of
655	C. kennedyi) falls. In a similar fashion, the presence of nannofossils of BC25 Zone, which are
656	elsewhere associated with middle Albian ammonites (Gale et al., 2011) are associated in the
657	Karai Section with ammonites of the upper Albian P. (S.) rostrata Zone. The mismatch between
658	ammonite and nannofossil zonal boundaries in the Cauvery Basin has been mentioned in
659	previous studies (e.g., Kale and Phansalkar, 1992b) but not discussed in any detail.
660	
661	The base of the Cenomanian stage is taken at the FO of the planktonic foraminifer,
662	Rotalipora globotruncanoides, which occurs in the uppermost Albian Ammonite Zone of
663	Arraphoceras briacensis, shortly beneath the first occurrence of ammonites of the lowermost
664	Cenomanian M. mantelli Zone (Kennedy et al., 2004). The base of NF Zone UC1 occurs within
665	the lowest part of this zone (Burnett, 1998).

In the Cauvery Basin, a discrepancy in the FO of *C. kennedyi* (NF Zone UC1) is noted with respect to the FO of lower Cenomanian *M. mantelli* Ammonite Zone fauna at Karai and Garudamangalam. In the Karai Section, *C. kennedyi* appears first at 301 m (sample KA301) and then occurs consistently from 337–448.04 m (sample KA337–KA448.04), after a gap of seven samples (sample KA305.5–KA332.5). In the Garudamangalam Section, *C. kennedyi* occurs consistently from its first appearance at 96.5 m (sample GM96.5) up to 159.5 m (sample GM159.5). The consistent occurrence of *C. kennedyi* observed at Garudamangalam can be equated with Karai (sample KA337–KA448.04), but the first appearance (sample KA 301) and
gap observed at Karai does not correlate with Garudamangalam (see distribution charts).
Overruling any possibility of caving in the Karai Section, it is reasonable to interpret that the
base of *C. kennedyi* at Garudamangalam could be truncated and, therefore, does not represent its
true base (Fig. 10b). Due to the observed variance, the FO of *C. kennedyi* was not employed to
delineate the base of the Cenomanian.

680

681 In view of the low stratigraphic occurrence of C.kennedvi at Karai, and the higher 682 occurrence at Garudamangalam, it is perhaps best to provisionally estimate the base of the 683 Cenomanian in the Cauvery Basin (Karai Section) a short distance beneath the first Cenomanian 684 ammonites (341.5 m, *M. mantelli* Ammonite Zone). The FOs of *G. ponticula* (332.5 m), small *G.* 685 cf. G. segmentatum and G. chiasta (328 m) are the closest nannofossil events that fall below the 686 first Cenomanian ammonites in the Karai Section (Fig. 9a). At Garudamangalam, the FO of G. 687 ponticula (53 m) and the FO and LO of G. chiasta (46 m and 53 m respectively) lie closest to the 688 base of the M. mantelli Ammonite Zone, facilitating the placement of the Albian-Cenomanian 689 boundary provisionally around 53m (Fig. 9b). The FO of G. ponticula is hereby proposed as a 690 new nannofossil proxy for the Albian-Cenomanian boundary. 691 692 The base of the Turonian in the Karai Section is taken at the base of NF Zone UC6, at a 693 significant hiatus. The base of UC6 Zone falls within the Watinoceras devonense Ammonite

Zone, which marks the base of the Turonian (Kennedy et al., 2005).

695

696 5.5. Palaeobiogeographic character of the Cauvery nannofossils

The good to moderate preservation of nannofossils in the Cauvery Basin makes it
possible to characterize the assemblages from a palaeobiogeographic perspective. The
nannofossil assemblages typically show high species richness of at least 50 species per sample,
and are generally dominated by cosmopolitan taxa, such as, *Biscutum, Chiastozygus, Eiffellithus, Lithraphidites, Retecapsa, Rhagodiscus, Staurolithites, Watznaueria*, and *Zeugrhabdotus* spp.

702

703 In order to make meaningful palaeobiogeographic comparisons, a sub-study was 704 undertaken in which Albian-Cenomanian samples from the Cauvery Basin were quantitatively 705 compared with coeval sections from onshore Europe (SE France: Col de Pré Guittard Section, 706 Mont Risou Section; S. England: BGS Selborne 1 & 2 boreholes, Folkestone-Warren Section) 707 and the Pacific Ocean (Hole 1213A, 17R–21R; 1214A, 7R–10R; 1207B, 25R–27R, ODP Leg 708 178, Shatsky Rise) (Kanungo, 2005). The Cauvery Basin nannofloras are very similar to those of 709 Europe and the Pacific region with the majority of taxa (85–90%) showing cosmopolitan 710 distribution across these regions. This indicates low provinciality during the mid-Cretaceous 711 (Albian-Cenomanian) interval, an observation that has also been confirmed by other studies, e.g., 712 Bown (2001) and Gale et al. (2011).

713

The term 'Austral' in this work refers to a southern high-latitude province recognised in the distribution of Cretaceous nannofossils (e.g., Watkins et al., 1996; Street and Bown, 2000; Lees, 2002). In general, high-latitude nannofossil assemblages typically show lower diversities than low-latitudes (Panera, 2012), but more specifically there are around three or four species/taxa that are reported to have exclusively Austral distribution during the Albian-Cenomanian interval (e.g., *S. falklandensis, Z. kerguelenensis*). The Cauvery Basin assemblages 720 exhibit a high-latitude character, evidenced by the consistent and common occurrence of 721 Repagulum parvidentatum and Seribiscutum primitivum, though more pronounced in the lower 722 Albian to lower Cenomanian section. Both of these taxa are well-known for their bipolar, high-723 latitude distribution in Boreal and Austral latitudes (Roth and Bowdler, 1981; Wise, 1983; 724 Mutterlose, 1992; Watkins et al., 1996; Street and Bown, 2000; Lees, 2002; McAnena et al., 725 2013, Kanungo et al., 2018). These two taxa gradually become rare and sporadically distributed 726 towards the upper part of the studied section (middle Cenomanian to lower Turonian) and can be 727 related to the late Cenomanian-late Turonian warming phase in the Indian Ocean, which resulted 728 in a southern shift in the Austral palaeobiogeographic zone (Lees, 2002). GPlates 729 palaeogeographic reconstructions show that the palaeolatitudinal position of the Cauvery Basin 730 did not change significantly through the study interval, being 45°45'S in the middle Albian (106 731 Ma), and 43°45'S in the early Turonian (93 Ma) (Matthews et al., 2016). The consistent presence 732 of Gartnerago spp. (G. chiasta, G. theta, G. segmentatum) and Octocyclus reinhardtii is a further 733 indication of the high-latitude character of these assemblages (e.g., Thierstein, 1981; Watkins et 734 al., 1996; Lees, 2002).

735

Two additional species, *Sollasites falklandensis* and *Zeugrhabdotus kerguelenensis*, have
been recognised as exclusively Austral taxa (Wise and Wind, 1977; Wise, 1983; Bralower and
Siesser, 1992; Herrle and Mutterlose, 2003; Panera, 2011), but they are rare in the Karai and
Garudamangalam sections. *Sollasites falklandensis* is found in just one sample (very rare) at
Karai and *Zeugrhabdotus kerguelenensis* is sporadically found at Garudamangalam. *S. falklandensis* was previously reported from the Dalmiapuram Grey Shale of the Cauvery Basin
(Bralower et al., 1993) and the southeastern Indian Ocean (Bralower et al., 1993). Z.

kerguelenensis, was initially described as a high-latitude species (Huber and Watkins, 1992;
Watkins et al., 1996) but later shown to be an Austral-Temperate taxon (Lees, 2002).
Nevertheless, it is dominantly an Austral taxon. The very rare occurrence of these taxa along
with the absence of other southern high-latitude taxa (e.g., *G. nanum, C. naturalisteplateauensis*)
indicate a relatively muted Austral character to the Cauvery nannofloras, with the assemblages
dominated by cosmopolitan taxa, and likely reflecting the moderately high-latitude setting of the
basin during the mid-Cretaceous interval.

750

751 A number of notable absences in the assemblages are also palaeobiogeographically 752 informative, including the Boreal taxa such as *Braloweria boletiformis*, *Ceratolithina bicornuta*, 753 and *Tegulalithus tessellatus* (Crux 1991; Bown et al., 1998). The absence of *Ceratolithina* spp. 754 (C. copis, C. duplex, C. naturalisteplateauensis) is perplexing because the genus has been 755 reported from a number of Indian Ocean sites (Lees, 2002). The Tethyan, neritic-adapted genus, 756 Nannoconus (Street and Bown, 2000) is also absent, but has been reported from the basin 757 previously. *Nannoconus (N. regularis and N. truittii)* is reported in quarry samples, but not from 758 the Karai-Kulakkalnattam and Garudamangalam outcrops (Jafar and Rai, 1989; Kale and 759 Phansalkar, 1992a, b; Kale et al., 2000). Similarly, the neritic taxon, Braarudosphaera (Roth and 760 Bowdler, 1981; Siesser et al; 1992; Kelly et al., 2003) is found in just one sample. The near 761 absence of *Braarudosphaera* and *Nannoconus* supports a more outer neritic palaeobathymetry 762 for the Karai Fm., an observation consistent with benthic foraminifera indicators (Nagendra et 763 al., 2013).

764

765 **6. Conclusions**

767 768	1.	Using the nannofossil zonation schemes of Bown et al. (1998) and Burnett (1998), the
769		age of two new Karai Fm. sections is established. The Karai Section is shown to be early
770		Albian (BC23 NF Zone) to early Turonian (UC6b NF Subzone) in age. The stratigraphic
771		range of the Garudamangalam Section is shorter, ranging from late Albian (BC27a
772		Subzone) to late Cenomanian (UC3e Subzone).
773		
774	2.	Overall, the applied nannofossil zonation schemes offer higher stratigraphic resolution
775		than earlier schemes, as they offer additional secondary markers/events that are
776		applicable in the Karai Fm. (e.g., FO of G. praeobliquum, LO of E. paragogus, LO of Z.
777		xenotus). The Albian (BC) zones of Bown et al. (1998) are all recognisable, whereas, the
778		Cenomanian (UC) zones of Burnett (1998) are only partially applicable. Zones UC2 (FO
779		of G. segmentatum) and UC4 (FO of C. biarcus) were not recognised. Several subzones
780		are, similarly, difficult to recognise, due to the rarity of markers (UC0c Subzone, FO of
781		C. anfractus), or inconsistencies in their stratigraphic order (e.g., UC1b Subzone, LO of
782		W. britannica), with respect to the zonation scheme of Burnett (1998).
783 784	3.	Two NF Zones, UC2 (lower Cenomanian, FO of G. segmentatum) and UC4 (upper
785		Cenomanian, FO of C. biarcus) are rendered unusable as zonal index markers. The
786		applicability of these markers is considered to be problematic due to their rarity or
787		inconsistency, rather than there being significantly missing stratigraphy in the basin.
788 789	4.	The application of <i>C. kennedyi</i> as a reliable indicator of the lower Cenomanian is
790		considered questionable due to a discrepancy observed in its first occurrence (FO) with
791		respect to the FO of lower Cenomanian ammonite fauna of the <i>M. mantelli</i> Zone at Karai

792		and Garudamangalam. This could, in part, be related to the non-preservation of
793		ammonites at key intervals in the basin, causing some of the observed mismatches
794		between the ammonite and nannofossil zones.
795 796	5.	The Albian-Cenomanian boundary interval appears to be continuous with the base of the
797		Cenomanian placed a short distance beneath the first Cenomanian ammonites of the M .
798		mantelli Ammonite Zone, which lies close to 341.5 m at Karai, and around 53 m at
799		Garudamangalam. The utility of additional bioevents such as the FO of G. ponticula
800		(proposed here as a new nannofossil proxy for the boundary), FO of G. chiasta, and the
801		LO of <i>E. paragogus</i> is helpful in delineating the boundary.
802		
803	6.	The Cenomanian-Turonian boundary interval is incomplete, indicated by the clustered
803 804	6.	The Cenomanian-Turonian boundary interval is incomplete, indicated by the clustered last occurrences of <i>A. albianus</i> , <i>H. chiastia</i> and <i>L. acutus</i> . A hiatus equivalent to Zone
	6.	
804	6.	last occurrences of A. albianus, H. chiastia and L. acutus. A hiatus equivalent to Zone
804 805	 6. 7. 	last occurrences of <i>A. albianus</i> , <i>H. chiastia</i> and <i>L. acutus</i> . A hiatus equivalent to Zone UC5 is present at Karai, representing ~0.66 Myrs.
804 805 806		last occurrences of <i>A. albianus</i> , <i>H. chiastia</i> and <i>L. acutus</i> . A hiatus equivalent to Zone UC5 is present at Karai, representing ~0.66 Myrs.
804 805 806 807		last occurrences of <i>A. albianus</i> , <i>H. chiastia</i> and <i>L. acutus</i> . A hiatus equivalent to Zone UC5 is present at Karai, representing ~0.66 Myrs. The nannoplankton assemblages are composed of broadly cosmopolitan taxa, despite the
804 805 806 807 808		last occurrences of <i>A. albianus, H. chiastia</i> and <i>L. acutus</i> . A hiatus equivalent to Zone UC5 is present at Karai, representing ~0.66 Myrs. The nannoplankton assemblages are composed of broadly cosmopolitan taxa, despite the high-latitude setting of southeastern India during the mid-Cretaceous. An Austral
804 805 806 807 808 809		 last occurrences of <i>A. albianus</i>, <i>H. chiastia</i> and <i>L. acutus</i>. A hiatus equivalent to Zone UC5 is present at Karai, representing ~0.66 Myrs. The nannoplankton assemblages are composed of broadly cosmopolitan taxa, despite the high-latitude setting of southeastern India during the mid-Cretaceous. An Austral character is indicated by the common and consistent presence of bipolar taxa such as <i>R</i>.
804 805 806 807 808 809 810		 last occurrences of <i>A. albianus</i>, <i>H. chiastia</i> and <i>L. acutus</i>. A hiatus equivalent to Zone UC5 is present at Karai, representing ~0.66 Myrs. The nannoplankton assemblages are composed of broadly cosmopolitan taxa, despite the high-latitude setting of southeastern India during the mid-Cretaceous. An Austral character is indicated by the common and consistent presence of bipolar taxa such as <i>R</i>. <i>parvidentatum</i> and <i>S. primitivum</i>, especially within the lower Albian to lower

814	strong Austral stamp, as typical Austral taxa (e.g., S. falklandensis, Z. kerguelenensis) are
815	very rare in the studied sections.

8. The early appearance of *C. hayi* in the early Albian, and *G. segmentatum* in the late
Albian in the Cauvery Basin suggests that these two species may have originated in
southern high-latitudes before migrating to northern regions.

820 Acknowledgements

821 This study formed a significant part of Sudeep Kanungo's Ph.D.; therefore, gratitude is

822 expressed to UCL's Graduate School funding and Alan Lord's support in obtaining those funds.

823 Special thanks are expressed to the following people for their invaluable assistance; Jackie Lees,

824 for her encouragement with nannofossil identifications; Ben Hathaway and Andy Gale's team for

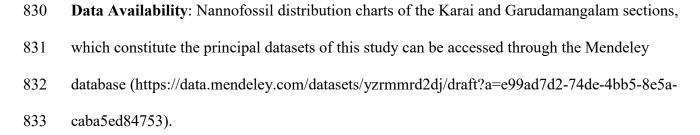
825 the laborious field sessions in India; Connor Nelson (EGI) for drafting figures; and Christopher

826 Kesler (EGI) for palaeo-map reconstructions. The careful recommendations made by two

827 anonymous reviewers, and the several deadline extensions granted by the editor-in-chief (E.

828 Koutsoukos) and Elena Jagt-Yazykova are gracefully acknowledged.

829



834

835 Supplementary Material: Appendix A (NF sample/slide list), Appendix B (Taxonomic list).
836

837	References	5

838	Acharyya, S. K., and Lahiri, T. C., 1991. Cretaceous palaeogeography of the Indian
839	subcontinent; a review. Cretaceous Research, 12, 3-26.
840	
841	Banerji, R. K., 1972. Stratigraphy and micropalaeontology of the Cauvery Basin, Part I. Exposed
842	area. Journal Palaeontological Society of India, 17, 1-24.
843	
844	Berrocoso, A. J., Huber, B. T., MacLeod, K. G., Petrizzo, M. R., Lees, J. A., Wendler, I., Coxall,
845	H., Mweneinda, A. K., Falzoni, F., Birch, H., Singano, J. M., Haynes, S., Cotton, L.,
846	Wendler, J., Bown, P. R., Robinson, S. A. and Gould, J., 2012. Lithostratigraphy,
847	biostratigraphy and chemostratigraphy of Upper Cretaceous and Paleogene sediments from
848	southern Tanzania: Tanzania Drilling Project Sites 27-35. Journal of African Earth Sciences,
849	70, 36-57.
850	
851	Bown, P. R. and Young, J. R., 1997. Mesozoic calcareous nannoplankton classification. Journal
852	of Nannoplankton Research, 19, 21-36.
853	
854	Bown, P. R. & Young, J. R., 1998. Techniques. In: Bown, P. R., (Ed.), Calcareous Nannofossil
855	Biostratigraphy. Kluwer Academic, 16-28.
856	
857	Bown, P. R., Rutledge, D. C., Crux, J. A. & Gallagher, L. T., 1998. Lower Cretaceous. In:
858	Bown, P. R., (Ed.), Calcareous Nannofossil Biostratigraphy. Kluwer Academic, 86-131.

860	Bown, P. R., 2001. Calcareous nannofossils of the Gault, Upper Greensand and Glauconitic Marl
861	(Middle Albian-Lower Cenomanian) from the BGS Selborne boreholes, Hampshire.
862	Proceedings of the Geologists' Association, 112, 223-236.
863	
864	Bralower, T. J. and Siesser, W. G., 1992. Cretaceous calcareous nannofossil biostratigraphy of
865	Sites 761, 762, and 763, Exmouth and Wombat plateaus, northwest Australia. Proceedings of
866	the Ocean Drilling Program, Scientific Results, 122, 529-556.
867	
868	Bralower, T. J., Sliter, W. V., Arthur, M. A., Leckie, R. M., Allard, D. & Schlanger, S. O., 1993.
869	Dysoxic/anoxic episodes in the Aptian-Albian (Early Cretaceous). Geophysical Monograph,
870	77, 5-37.
871	
872	Bralower, T. J., Leckie, R. M., Sliter, W. V. and Thierstein, H. R., 1995. An integrated
873	Cretaceous microfossil biostratigraphy. In: W. A. Berggren, D. V. Kent, MP. Aubry and J.
874	Hardenbol (Eds.), Geochronology Time Scales and Global Stratigraphic Correlation, SEPM
875	Special Publication No. 54, 65-79.
876	
877	Bralower, T. J. and Bergen, J. A., 1998. Cenomanian-Santonian calcareous nannofossil
878	biostratigraphy of a transect of cores drilled across the Western Interior Seaway. In:
879	Stratigraphy and Paleoenvironments of the Cretaceous Western Interior Seaway, USA.
880	SEPM Concepts in Sedimentology and Paleontology No.6, 59-77. ISBN I-56576-044-1.
881	

882	Burnett, J. A., 1998. Upper Cretaceous. In: P. R. Bown (Ed.), Calcareous Nannofossil
883	Biostratigraphy. Kluwer Academic, 132-199.
884	
885	Corbett, M. J. and Watkins, D. K., 2013. Calcareous nannofossil paleoecology of the mid-
886	Cretaceous Western Interior Seaway and evidence of oligotrophic surface waters during
887	OAE2. Palaeogeography, Palaeoclimatology, Palaeoecology, 392, 510-523.
888	http://dx.doi.org/10.1016/j.palaeo.2013.10.1007
889	
890	Crux, J. A., 1991. Albian calcareous nannofossils from the Gault Clay of Munday's Hill
891	(Bedfordshire, England). Journal of Micropalaeontology, 10, 203-221.
892	
893	Directorate General of Hydrocarbons (DGH), 2018. Cauvery Basin (Basin Information), online
894	document (accessed on 20.11.2018)
895	http://dghindia.gov.in//assets/downloads/56cfe94a4c105The_Cauvery_Basin.pdf
896	
897	Gale, A. S., Kennedy, W. J., Burnett, J. A., Caron, M. and Kidd, B. E., 1996. The Late Albian to
898	Early Cenomanian succession at Mont Risou near Rosans (Drôme, SE France): an integrated
899	study (ammonites, inoceramids, planktonic foraminifera, nannofossils, oxygen and carbon
900	isotopes). Cretaceous Research, 17, 515-606.
901	
902	Gale, A. S., Hardenbol, J., Hathway, B., Kennedy, W. J., Young, J. R., and Phansalkar, V., 2002.
903	Global correlation of Cenomanian (Upper Cretaceous) sequences: Evidence for Milankovitch
904	control on sea level. Geology, 30 (4), 291-294.

906	Gale, A. S., Bown, P., Caron, M., Crampton, J., Crowhurst, S. J., Kennedy, W. J., Petrizzo, M.
907	R. and Wray, D. S., 2011. The uppermost Middle and Upper Albian succession at the Col de
908	Palluel, Hautes-Alpes, France: An integrated study (ammonites, inoceramid bivalves,
909	planktonic foraminifera, nannofossils, geochemistry, stable oxygen and carbon isotopes,
910	cyclostratigraphy). Cretaceous Research, 32, 59-130.
911	
912	Gale, A. S., Kennedy, W. J. and Walaszczyk, 2019. Upper Albian, Cenomanian and Lower
913	Turonian stratigraphy, ammonite and inoceramid bivalve faunas from the Cauvery Basin,
914	Tamil Nadu, South India. Acta Geologica Polonica, 69 (2), 161-338.
915	
916	Govindan, A., Ravindran, C. N. and Rangaraju, M. K., 1996. Cretaceous stratigraphy and
917	planktonic foraminiferal zonation of Cauvery basin, South India. In: Sahni, A. (Ed.),
918	Cretaceous stratigraphy and palaeoenvironments. Memoir Geological Society of India, 37,
919	155-187.
920	
921	Govindan, A., Ananthanarayanan, S. and Vijayalakshmi, K. G., 2000. Cretaceous petroleum
922	system in Cauvery Basin, India. In: Govindan, A. (Ed.), Cretaceous Stratigraphy - An
923	Update. Memoir Geological Society of India, 46, 365-382.
924	
925	Hart, M. B., Joshi, A. and Watkinson, M. P., 2001. Mid-Late Cretaceous stratigraphy of the
926	Cauvery Basin and the development of the eastern Indian Ocean. Journal Geological Society
927	of India, 58, 217-229.

929	Herrle, J. O. and Mutterlose, J., 2003. Calcareous nannofossils from the Aptian-early Albian of
930	SE France: paleoecological and biostratigraphic implications. Cretaceous Research, 24, 1-22.
931	
932	Holmes, M. A. and Watkins, D. K., 1992. Middle and Late Cretaceous history of the Indian
933	Ocean. Synthesis of results from scientific drilling in the Indian Ocean, Geophysical
934	Monograph, 70, 225-244.
935	
936	Huber, B. T. and Watkins, D. K., 1992. Biogeography of Campanian-Maastrichtian calcareous
937	plankton in the region of the Southern Ocean: paleogeographic and paleoclimatic
938	implications. In: The Antarctic paleoenvironment: a perspective on global change. Antarctic
939	Research Series, 56, 31-60.
940	
941	Jafar, S. A., and Rai, J., 1989. Discovery of Albian nannoflora from type Dalmiapuram
942	Formation, Cauvery Basin, India – paleoceanographic remarks. Current Science, 58 (7), 358-
943	363.
944	
945	Kale, A. S., and Phansalkar, V. G., 1992a. Calcareous nannofossils from the Utatur Group,
946	Trichinopoly district, Tamil Nadu, India. Journal Palaeontological Society of India, 37, 85-
947	102.
948	
949	Kale, A. S., and Phansalkar, V. G., 1992b. Nannofossil biostratigraphy of the Utatur Group,
950	Trichinopoly district, South India. Memorie di Scienze Geologiche, XLIII, 89-107.

952	Kale, A. S., Lotfalikani, A., and Phansalkar, V. G., 2000. Calcareous nannofossils from the
953	Uttatur Group of Trichinopoly Cretaceous, South India. Memoir Geological Society of India,
954	46, 213-227.
955	
956	Kanungo, S., 2005. Biostratigraphy and palaeoceanography of mid-Cretaceous calcareous
957	nannofossils: studies from the Cauvery Basin, SE India; the Gault Clay Formation, SE
958	England; ODP Leg 171B, western North Atlantic and ODP Leg 198, northwest Pacific
959	Ocean. Unpublished PhD thesis. University College London, 260 pp.
960	
961	Kanungo, S., Bown, P. R., Young, J. R. and Gale, A. S., 2018. A brief warming event in the late
962	Albian: evidence from calcareous nannofossils, macrofossils, and isotope geochemistry of
963	the Gault Clay Formation, Folkestone, southeastern England. Journal of Micropalaeontology,
964	37, 231-247. https://doi.org/10.5194/jm-37-231-2018
965	
966	Kelly, D. C., Norris, R. D. and Zachos, J. C., 2003. Deciphering the paleoceanographic
967	significance of Early Oligocene Braarudosphaera chalks in the South Atlantic. Marine
968	Micropaleontology, 49, 49-63.
969	
970	Kennedy, W. J., Gale, A. S., Bown, P. R., Caron, M., Davey, R. J., Gröcke, D., Wray, D. J.,
971	2000. Integrated stratigraphy across the Aptian-Albian boundary in the Marnes Bleues, at the
972	Col de Pré-Guittard, Aryanon (Drôme), and at Tartonne (Alpes-de-Haute-Provence), France:

973	a candidate Global Boundary Stratotype Section and Point for the base of the Albian stage.
974	Cretaceous Research, 21, 591-720.
975	
976	Kennedy, W. J., Gale, A. S., Lees, J. A. and Caron, M., 2004. The Global Boundary Stratotype
977	Section and Point (GSSP) for the base of the Cenomanian Stage, Mont Risou, Hautes-Alpes,
978	France. Episodes Journal of International Geoscience, 27 (1), 21-32.
979	
980	Kennedy, W. J., Walaszczyk, I. and Cobban, W. A., 2005. The Global Boundary Stratotype
981	Section and Point for the base of the Turonian stage of the Cretaceous: Pueblo, Colorado.
982	Episodes, 28, 93-104.
983	
984	Kennedy, W. J., Gale, A. S., Huber, B. T., Petrizzo, M. R., Bown, P. R., Barchetta, A. and
985	Jenkyns, H. C., 2014. Integrated stratigraphy across the Aptian/Albian boundary at Col de
986	Pré-Guittard (southeast France): A candidate Global Boundary Stratotype Section.
987	Cretaceous Research, 51, 248-259. https://doi.org/10.1016/j.cretres.2014.06.005
988	
989	
990	Lees, J. A., 2002. Calcareous nannofossil biogeography illustrates palaeoclimate change in the
991	Late Cretaceous Indian Ocean. Cretaceous Research, 23, 537-634.
992	

993	Lees, J. A. and Bown, P. R., 2005. Upper Cretaceous calcareous nannofossil biostratigraphy,
994	ODP Leg 198 (Shatsky Rise, northwest Pacific Ocean). In: Bralower, T. J., Premoli Silva, I.,
995	and Malone, M. J., (Eds.), Proceedings of the ODP, Scientific Results, 198, 1-60
996	
997	Matthews, K. J., Maloney, K. T., Zahirovic, S., Williams, S. E., Seton, M., and Müller, R. D.,
998	2016, Global plate boundary evolution and kinematics since the late Paleozoic: Global and
999	Planetary Change, doi: 10.1016/j.gloplacha.2016.10.002.
1000	
1001	McAnena, A., Flögel, S., Hofmann, P., Herrle, J. O., Griesand, A., Pross, J., Talbot, H. M.,
1002	Rethemeyer, J., Wallmann, K. and Wagner, T., 2013. Atlantic cooling associated with a
1003	marine biotic crisis during the mid-Cretaceous period. Nature Geoscience, 6, 558-561,
1004	http://doi.org/ 10.1038/NGEO1850.
1005	
1006	Mutterlose, J. 1992. Biostratigraphy and palaeobiogeography of Early Cretaceous calcareous
1007	nannofossils. Cretaceous Research, 13, 167-189.
1008	
1009	Narayanan, V., 1977. Biozonation of the Uttatur Group, Trichinopoly, Cauvery Basin. Journal of
1010	the Geological Society of India, 18 (8), 415-428.
1011	
1012	Nagendra, R., Kamalak Kannan, B. V., Sen, G., Gilbert, H., Bakkiaraj, D., Nallapa Reddy, A.
1013	and Jaiprakash, B. C., 2011. Sequence surfaces and paleobathymetric trends in Albian to
1014	Maastrichtian sediments of Ariyalur area, Cauvery Basin, India. Marine and Petroleum
1015	Geology, 28, 895-905.

Nagendra, R., Sathiyamoorthy, P., Pattanayak, S., Nallapa Reddy, A. and Jaiprakash, B. C.,
2013. Stratigraphy and paleobathymetric interpretation of the Cretaceous Karai Shale
Formation of Uttatur Group, Tamil Nadu, India. Stratigraphy and Geological Correlation, 21
(7), 675-688, doi: 10/1134/S0869593813070046.

1021

Nagendra, R. and Nallapa Reddy, A., 2017. Major geologic events of the Cauvery Basin, India
and their correlation with global signatures – A review. Journal of Palaeogeography, 6 (1),
69-83.

1025

Ogg, J. G. and Hinnov, L. A., 2012. Cretaceous. *In:* F. M. Gradstein, J. G. Ogg, M. D. Schmitz
and G. M. Ogg (Eds.), *The Geologic Time Scale 2012* – Volume 2. Elsevier, 793-855.

1028

1029 Pérez Panera, J. P., 2011. The calcareous nannofossil *Sollasites falklandensis*1030 (Coccolithophyceae) and its biostratigraphic and palaeoceanographic importance in the
1031 Albian of the Austral Basin, Argentina. Cretaceous Research, 32, 723-737.

1032

Pérez Panera, J. P., 2012. Two new heterococcoliths from the Albian-Cenomanian, Austral
Basin, Patagonia, Argentina. Journal of Nannoplankton Research, 32 (2), 75-78.

1035

1036 Paranjape, A. R., Kale, A. S. and Kulkarni, K. G., 2013. Uttatur-Trichinopoly Group contact,

1037 Cauvery Basin: A sequence stratigraphic perspective. *In*: Abstract volume of the 24th Indian

1038 Colloquium on Micropalaeontology and Stratigraphy, Dehradun, 90-91.

1040	Paranjape. A. R., Kulkarni, K. G. and Kale, A. S., 2015. Sea level changes in the upper Aptian-
1041	lower/middle (?) Turonian sequence of Cauvery Basin, India – An ichnological perspective.
1042	Cretaceous Research, 56, 702-715.
1043	
1044	Perch-Nielsen, K., 1979. Calcareous nannofossils from the Cretaceous between the North Sea
1045	and the Mediterranean. In: Aspekte der Kreide Europas, IUGS Series A 6, 223-272.
1046	
1047	Perch-Nielsen, K., 1985. Mesozoic calcareous nannofossils. In: H. M. Bolli, J. B. Saunders and
1048	K. Perch-Nielsen (Eds.), Plankton Stratigraphy. Cambridge University Press, Cambridge,
1049	329-426.
1050	
1051	Powell, C. McA., Roots, S. R. and Veevers, J. J., 1988. Pre-breakup continental extension in East
1052	Gondwanaland and the early opening of the eastern Indian Ocean. Tectonophysics, 155, 261-
1053	283.
1054	
1055	Prabhakar, K. N. and Zutshi, P. L., 1993. Evolution of the southern part of Indian east coast
1056	basins. Journal Geological Society of India, 41, 215-230.
1057	
1058	Raju, D. S. N., Ravindran, C. N., Mishra, P. K. and Singh, J., 1991. Cretaceous and Cenozoic
1059	foraminiferal zonation framework for east coast sedimentary basins of India. Geoscience
1060	Journal, 12, 155-175.
1061	

1062	Raju, D. S. N., Ravindran, C. N. and Kalyansundar, R., 1993. Cretaceous cycles of sea level
1063	changes in the Cauvery Basin, India – a first revision. Bulletin of the Oil and Natural Gas
1064	Commission, 30, 101-113.
1065	
1066	Ramkumar, M., Stüben, D. and Berner, Z., 2004. Lithostratigraphy, depositional history and sea
1067	level changes of the Cauvery Basin, southern India. Annals of Geology of Balkan Peninsula,
1068	65, 1-27.
1069	
1070	Ramkumar, M., Stüben, D. and Berner, Z., 2011. Barremian-Danian chemostratigraphic
1071	sequences of the Cauvery Basin, India: Implications on scales of stratigraphic correlation.
1072	Gondwana Research, 19, 291-309, doi:10.1016/j.gr.2010.05.014.
1073	
1074	Rao, M. V., Chidambaram, L., Bharktya, D. and Janardhanan, M., 2010. Integrated analysis of
1075	late Albian to middle Miocene sediments in Gulf of Mannar shallow waters of the Cauvery
1076	Basin, India: a sequence stratigraphic approach. Conference Proceedings of the 8th Biennial
1077	International Conference and Exposition on Petroleum Geophysics, Hyderabad, pp. 1-9.
1078	
1079	Roth, P. H., 1978. Cretaceous nannoplankton biostratigraphy and oceanography of the
1080	northwestern Atlantic Ocean. Initial reports of the DSDP, 44, 731-760.
1081	
1082	Roth, P. H. and Bowdler, J. K., 1981. Middle Cretaceous calcareous nannoplankton
1083	biogeography and oceanography of the Atlantic Ocean. Society of Economic Paleontologists and
1084	Mineralogists (SEPM), Special Publication, 32, 517-546.

1085	Sastri, V. V., Venkatachala, B. S. and Narayanan, V., 1981. The evolution of the east coast of
1086	India. Palaeogeography, Palaeoclimatology, Palaeoecology, 36, 23-54.
1087	
1088	Silva Jr., R., Rios-Netto, A. M., Silva, S. C., Valle, B., Borghi, L. and Abbots-Queiroz, F., 2020.
1089	Middle Cretaceous calcareous nannofossils from the cored well UFRJ-2-LRJ-01-SE,
1090	Sergipe-Alagoas Basin, Brazil: New biostratigraphy and paleobiogeographic inferences.
1091	Cretaceous Research, 106, 1-12. https://doi.org/10.1016/j.cretres.2019.104245
1092	
1093	Siesser, W. G., Bralower, T. J. and De Carlo, E. H., 1992. Mid-Tertiary Braarudosphaera-rich
1094	sediments on the Exmouth Plateau. Proceedings of the Ocean Drilling Program, Scientific
1095	Results, 122, 653-663.

1097 Sissingh, W., 1977. Biostratigraphy of Cretaceous calcareous nannoplankton. Geologie en
1098 Mijnbouw, 56, 37-65.

1099

- 1100 Street, C. and Bown, P.R., 2000. Palaeobiogeography of Early Cretaceous (Berriasian-
- 1101 Barremian) calcareous nannoplankton. Marine Micropaleontology, 39, 265-291.

1102

Sundaram, R. and Rao, P. S., 1986. Lithostratigraphy of Cretaceous and Palaeocene rocks of
Tiruchirapalli district, Tamil Nadu, South India. Records of the Geological Survey of India,
1105 116, 11-23.

1107	Sundaram, R., Henderson, R. A., Ayyasami, K. and Stilwell, J. D., 2001. A lithostratigraphic
1108	revision and palaeoenvironmental assessment of the Cretaceous system exposed in the
1109	onshore Cauvery Basin, southern India. Cretaceous Research, 22, 743-762.
1110	
1111	Tewari, A., Hart, M. B. and Watkinson, M. P., 1996a. A revised lithostratigraphic classification
1112	of the Cretaceous rocks of the Trichinopoly District, Cauvery Basin, southeast India.
1113	Contributions XV Indian Colloquium of Micropalaeontology and Stratigraphy, Dehra Dun
1114	(Eds. J. Pandey, R. J. Azmi, A. Bhandari and A. Dave), 789-800.
1115	
1116	Tewari, A., Hart, M. B. and Watkinson, M. P., 1996b. Foraminiferal recovery after the mid-
1117	Cretaceous oceanic anoxic events (OAEs) in the Cauvery Basin, southeast India. In: M. B.
1118	Hart (Ed.), Biotic Recovery from Mass Extinction Events. Geological Society Special
1119	Publication No. 102, 237-244.
1120	
1121	
1122	Thierstein, H. R., 1981. Late Cretaceous nannoplankton and the change at the Cretaceous-
1123	Tertiary boundary. Society of Economic Paleontologists and Mineralogists (SEPM), Special
1124	Publication, 32, 355-394.
1125	
1126	Veevers, J. J., Powell, C. McA. and Roots, D., 1991. Review of the seafloor spreading around
1127	Australia, 1. Synthesis of the pattern of spreading. Australian Journal of Earth Sciences, 38,
1128	373-389.
1129	

1130	Venkatachalapathy, R. and Ragothaman, V., 1995a. Palaeo-ecology of mid-Cretaceous
1131	foraminifera in the Cauvery Basin, east coast of India. Journal of the Palaeontological
1132	Society of India, 40, 9-20.
1133	
1134	Venkatachalapathy, R. and Ragothaman, V., 1995b. A foraminiferal zonal scheme for the mid-
1135	Cretaceous sediments of the Cauvery Basin, India. Cretaceous Research, 16, 415-433.
1136	
1137	Venkatachalapathy, R., Harini, L., Arun Bharathi, V., Bragin, N., Bragina, L. G. and Oleg, K.,
1138	2014. Foraminiferal and radiolarian assemblages in the late Albian-early Cenomanian
1139	sediments of Karai Shale, Tamil Nadu. International Journal of Geology, Earth &
1140	Environmental Sciences (online), 4 (1), 250-265, http://www.cibtech.org/jgee.htm
1141	
1142	Watkins, D. K., Wise, S. W., Pospichal, J. J. and Crux, J., 1996. Upper Cretaceous calcareous
1143	nannofossil biostratigraphy and paleoceanography of the Southern Ocean. In: A.
1144	Moguilevsky and R. Whatley (Eds.), Microfossils and oceanic environments, pp. 355-381
1145	(University of Wales, Aberystwyth Press, Aberystwyth).
1146	
1147	Watkinson, M. P., Hart, M. B. and Joshi, A., 2007. Cretaceous tectonostratigraphy and the
1148	development of the Cauvery Basin, southeast India. Petroleum Geoscience, 13, 181-191.
1149	
1150	Wise, S. W., 1983. Mesozoic and Cenozoic calcareous nannofossils recovered by DSDP Leg 71
1151	in the Falkland Plateau region, Southwest Atlantic Ocean. Initial Reports of the Deep Sea
1152	Drilling Project, 71, 481-550.

1153 1154	Wise, S. W. and Wind, F. H., 1977. Mesozoic and Cenozoic calcareous nannofossils recovered
1155	by DSDP Leg 36 drilling on the Falkland Plateau, southwest Atlantic sector of the Southern
1156	Ocean. Initial reports of the DSDP, 36, Washington (U. S. Govt. Printing Office), 269-491.
1157	
1158	Young, J. R., Bergen, J. A., Bown, P. R., Burnett, J. A., Fiorentino, A., Jordan, R. W., Kleijne,
1159	A., van Niel, B. E., Ton Romein, A. J., and von Salis, K., 1997. Guidelines for coccolith and
1160	calcareous nannofossil terminology. Palaeontology, 40, 875-912.
1161	
1162	Young, J. R., Bown P. R. and Lees, J. A., 2017. Nannotax3 website. International
1163	Nannoplankton Association (2017). http://www.mikrotax.org/Nannotax3/
1164 1165 1166 1167	Table Captions (4 tables)
1168	Table 1. Nannofossil zone and subzone markers recognised in the Karai Section, Karai Fm. (in
1169	stratigraphic order).
1170	
1171	Table 2. Nannofossil zone and subzone markers recognised in the Garudamangalam Section,
1172	Karai Fm. (in stratigraphic order).
1173	
1174	Table 3. Summary (presence/absence) of Cenomanian zone and subzone markers in the Karai
1175	and Garudamangalam sections, Cauvery Basin, compared with their occurrences reported in
1176	Burnett (1998) and Lees (2002).
1177	

	Table 4 . Relative stratigraphic order of nannofossil events around the Albian-Cenomanian
1179	boundary interval in the Cauvery Basin and Mont Risou GSSP in SE France (Gale et al., 1996).
1180	
1181 1182	Figures Captions (10 figures, Figures 1–3 and Figure 9a, b are in colour)
1183	Figure 1. Location map of (A) Cauvery Basin, and (B) Karai and Garudamangalam sections
1184	(Pondicherry Sub-Basin) in Tamil Nadu, SE India.
1185	
1186	Figure 2. Lithostratigraphic division and stratigraphic position of the Uttatur Group and Karai
1187	Fm., onshore Cauvery Basin, SE India (modified after Paranjape et al., 2015).
1188	
1189	Figure 3. Palaeogeographic reconstruction of the Cauvery Basin in the middle Albian (106 Ma)
1190	and early Turonian (93 Ma) using GPlates (Matthews et al., 2016).
1191	
1192	Figure 4. Nannofossil species recorded in the Karai Fm., Karai and Garudamangalam sections
1193	
	(scale bar 2 µm). 1, Chiastozygus litterarius, sample KA377.5 (KA377.5-NF/SK). 2,
1194	(scale bar 2 μm). 1, <i>Chiastozygus litterarius</i> , sample KA377.5 (KA377.5-NF/SK). 2, <i>Chiastozygus platyrhethus</i> , sample KA314.5 (KA314.5-NF/SK). 3–5, <i>Chiastozygus spissus</i> ,
1194 1195	
	Chiastozygus platyrhethus, sample KA314.5 (KA314.5-NF/SK). 3–5, Chiastozygus spissus,
1195	<i>Chiastozygus platyrhethus</i> , sample KA314.5 (KA314.5-NF/SK). 3–5, <i>Chiastozygus spissus</i> , sample GM72.5, (GM72.5-NF/SK). 6–7, <i>Chiastozygus trabalis</i> , sample GM102.5 (GM102.5-
1195 1196	<i>Chiastozygus platyrhethus</i> , sample KA314.5 (KA314.5-NF/SK). 3–5, <i>Chiastozygus spissus</i> , sample GM72.5, (GM72.5-NF/SK). 6–7, <i>Chiastozygus trabalis</i> , sample GM102.5 (GM102.5-NF/SK). 8, <i>Loxolithus armilla</i> , sample KA350.5 (KA350.5-NF/SK). 9–12, <i>Loxolithus bicyclus</i> ,
1195 1196 1197	<i>Chiastozygus platyrhethus</i> , sample KA314.5 (KA314.5-NF/SK). 3–5, <i>Chiastozygus spissus</i> , sample GM72.5, (GM72.5-NF/SK). 6–7, <i>Chiastozygus trabalis</i> , sample GM102.5 (GM102.5-NF/SK). 8, <i>Loxolithus armilla</i> , sample KA350.5 (KA350.5-NF/SK). 9–12, <i>Loxolithus bicyclus</i> , n. sp., (9) HOLOTYPE, (11) PARATYPE, 11–12 same specimen, sample GM101 (GM101-
1195 1196 1197 1198	<i>Chiastozygus platyrhethus</i> , sample KA314.5 (KA314.5-NF/SK). 3–5, <i>Chiastozygus spissus</i> , sample GM72.5, (GM72.5-NF/SK). 6–7, <i>Chiastozygus trabalis</i> , sample GM102.5 (GM102.5-NF/SK). 8, <i>Loxolithus armilla</i> , sample KA350.5 (KA350.5-NF/SK). 9–12, <i>Loxolithus bicyclus</i> , n. sp., (9) HOLOTYPE, (11) PARATYPE, 11–12 same specimen, sample GM101 (GM101-NF/SK). 13–14, <i>Staurolithites</i> cf. <i>S. angustus</i> , sample KA171 (KA171-NF/SK). 15–16,

- 1202 sample GM56 (GM56-NF/SK). 23–25, Staurolithites sp., sample GM75.5 (GM75.5-NF/SK). 26,
- 1203 Tranolithus orionatus, sample KA157.5 (KA157.5-NF/SK). 27–29, Tranolithus simplex, n. sp.,
- 1204 (27) HOLOTYPE, sample KA373, (KA373-NF/SK). 30–32, *T. simplex*, n. sp., (30)
- 1205 PARATYPE, sample GM37 (GM37-NF/SK). 33, Tranolithus gabalus, sample KA157.5
- 1206 (KA157.5-NF/SK). 34, Zeugrhabdotus bicrescenticus, sample KA445.7 (KA445.7-NF/SK). 35,
- 1207 Zeugrhabdotus diplogrammus, sample KA373 (KA373-NF/SK). 36–37, Zeugrhabdotus
- 1208 kerguelenensis (side view), sample GM65 (GM65-NF/SK). 38–39, Zeugrhabdotus cf. Z.
- 1209 embergeri, sample GM81.5 (GM81.5-NF/SK). 40, Zeugrhabdotus howei, sample KA469.1
- 1210 (KA469.1-NF/SK). 41, Z. howei, sample KA445.7 (KA445.7-NF/SK). 42, Zeugrhabdotus
- 1211 *noeliae*, sample KA157.5 (KA157.5-NF/SK).
- 1212
- 1213 Figure 5. Nannofossil species recorded in the Karai Fm., Karai and Garudamangalam sections
- 1214 (scale bar 2 μm). 1, Zeugrhabdotus noeliae, sample KA157.5 (KA157.5-NF/SK). 2–3,
- 1215 Zeugrhabdotus xenotus, sample KA287.5 (KA287.5-NF/SK). 4, Amphizygus brooksii, sample
- 1216 KA428.5 (KA428.5-NF/SK). 5, *Eiffellithus gorkae*, sample KA469.1 (KA469.1-NF/SK). 6,
- 1217 Eiffellithus turriseiffelii, sampleGM19 (GM19-NF/SK). 7–8, Eiffellithus vonsalisiae, sample
- 1218 GM113 (GM113-NF/SK). 9–11, Eiffellithus monechiae, sample KA180 (KA180-NF/SK). 12–
- 1219 13, Zeugrhabdotus clarus, sample GM31 (GM31-NF/SK). 14, Helicolithus compactus, sample
- 1220 KA464.2 (KA464.2-NF/SK). 15, Helicolithus trabeculatus, sample KA180 (KA180-NF/SK). 16,
- 1221 *Tegumentum stradneri*, sample GM49 (GM49-NF/SK). 17, *Percivalia fenestrata*, sample GM22
- 1222 (GM22-NF/SK). 18, P. fenestrata, sample GM86 (GM86-NF/SK). 19–20, Rhagodiscus
- 1223 achlyostaurion, sample GM56 (GM56-NF/SK). 21, Rhagodiscus asper, sample KA445.7
- 1224 (KA445.7-NF/SK). 22–23, R. asper (large), sample KA22.5 (KA22.5-NF/SK). 24, Rhagodiscus

- 1225 infinitus, sample KA153 (KA153-NF/SK). 25–26, Rhagodiscus hamptonii, sample GM28
- 1226 (GM28-NF/SK). 27, Rhagodiscus gallagheri, sample KA445.7 (KA445.7-NF/SK). 28, R.
- 1227 gallagheri, sample GM10 (GM10-NF/SK). 29, Rhagodiscus reniformis, sample GM113
- 1228 (GM113-NF/SK). 30, *Rhagodiscus splendens*, sample KA459.3 (KA459.3-NF/SK). 31–32,
- 1229 Corollithion kennedyi, sample GM96.5 (GM96.5-NF/SK). 33–34, Helicolithus leckiei, sample
- 1230 GM113 (GM113-NF/SK). 35, Corollithion exiguum, sample KA459.3 (KA459.3-NF/SK). 36,
- 1231 Corollithion protosignum, sample KA135 (KA135-NF/SK). 37, Corollithion signum, sample
- 1232 GM59 (GM59-NF/SK). 38–39, Rotelapillus laffittei, sample KA459.3 (KA459.3-NF/SK). 40,
- 1233 Stoverius achylosus, sample KA464.2 (KA464.2-NF/SK). 41–42, Cylindralithus biarcus, sample
- 1234 KA464.2 (KA464.2-NF/SK).
- 1235
- 1236 Figure 6. Nannofossil species recorded in the Karai Fm., Karai and Garudamangalam sections
- 1237 (scale bar 2 µm). 1, Cylindralithus nudus, sample KA305.5 (KA305.5-NF/SK). 2, C. nudus (side
- 1238 view), sample GM62 (GM62-NF/SK). 3-4, Cylindralithus sculptus, sample KA445.7 (KA445.7-
- 1239 NF/SK). 5–6, Cylindralithus serratus, sample GM78.5 (GM78.5-NF/SK). 7–8, Axopodorhabdus
- 1240 *albianus*, sample KA180 (KA180-NF/SK). 9–10, *Cribrosphaerella ehrenbergii*, sample GM59
- 1241 (GM59-NF/SK). 11–12, Hemipodorhabdus cf. H. gorkae, sample GM37 (GM37-NF/SK). 13,
- 1242 Tetrapodorhabdus decorus, sample KA 445.7 (KA445.7-NF/SK). 14, Octocyclus reinhardtii,
- 1243 sample KA469.1 (KA469.1-NF/SK). 15, Biscutum constans, sample KA445.7 (KA445.7-
- 1244 NF/SK). 16, B. constans (large), sample GM113 (GM113-NF/SK). 17, Seribiscutum primitivum,
- 1245 sample GM0 (GM0-NF/SK). 18, S. primivitum, sample KA433 (KA433-NF/SK). 19–20,
- 1246 Crucibiscutum hayi, sample GM0 (GM0-NF/SK). 21–22, Sollasites falklandensis, sample
- 1247 KA22.5 (KA22.5-NF/SK). 23, Prediscosphaera columnata (small, circular), sample KA180

- 1248 (KA180-NF/SK). 24, P. columnata (subcircular), sample GM81.5 (GM81.5-NF/SK). 25, P.
- 1249 columnata (large), sample GM89 (GM89-NF/SK). 26, Prediscosphaera cretacea, sample
- 1250 GM102.5 (GM102.5-NF/SK). 27–28, Prediscosphaera cf. P. ponticula, sample GM113
- 1251 (GM113-NF/SK). 29, Prediscosphaera spinosa, sample GM113 (GM113-NF/SK). 30, P.
- 1252 spinosa, sample GM53 (GM53-NF/SK). 31, Cretarhabdus conicus, sample KA457.4 (KA457.4-
- 1253 NF/SK). 32, Cretarhabdus striatus, sample KA323.5 (KA323.5-NF/SK). 33–35, Cretarhabdus
- 1254 multicavus, sample GM19 (GM19-NF/SK). 36, Flabellites oblongus, sample KA85.5 (KA85.5-
- 1255 NF/SK). 37, Helenea chiastia, sample KA368.5 (KA368.5-NF/SK). 38–39, Retecapsa cf. R.
- 1256 angustiforata, sample KA448.9 (KA448.9-NF/SK). 40, Retecapsa surirella, sample GM72.5
- 1257 (GM72.5-NF/SK). 41, Tubodiscus burnettiae, sample KA85.5 (KA85.5-NF/SK). 42, Manivitella
- 1258 *pemmatoidea*, sample KA274 (KA274-NF/SK).
- 1259
- 1260 Figure 7. Nannofossil species recorded in the Karai Fm., Karai and Garudamangalam sections
- 1261 (scale bar 2 µm). 1, Manivitella fibrosa, n. sp., sample K274 (KA274-NF/SK). 2, M. fibrosa, n.
- 1262 sp., HOLOTYPE, sample KA278.5 (KA278.5-NF/SK). 3, *M. fibrosa*, n. sp., sample GM65
- 1263 (GM65-NF/SK). 4, *M. fibrosa*, n. sp., PARATYPE, sample KA391 (KA391-NF/SK). 5–6, *M.*
- 1264 *fibrosa*, n. sp., sample KA292 (KA292-NF/SK). 7, *Watznaueria barnesiae*, sample KA451.9
- 1265 (KA451.9-NF/SK). 8, Watznaueria biporta, sample KA469.1 (KA469.1-NF/SK). 9, Watznaueria
- 1266 britannica, sample GM49 (GM49-NF/SK). 10, Watznaueria ovata, sample GM65 (GM65-
- 1267 NF/SK). 11–12, Broinsonia enormis, sample KA 451.9 (KA451.9-NF/SK). 13–14, Broinsonia
- 1268 galloisii, GM22 (GM22-NF/SK). 15–16, Broinsonia matalosa, sample KA386.5 (KA386.5-
- 1269 NF/SK). 17–19, Gartnerago stenostaurion, sample KA292 (KA292-NF/SK). 20–22, Broinsonia
- 1270 cf. B. viriosa, sample KA85.5 (KA85.5-NF/SK). 23, Crucicribrum anglicum, sample KA220,

- 1271 (KA220-NF/SK). 24–25, Gartnerago chiasta, sample GM46 (GM46-NF/SK). 26–27,
- 1272 Gartnerago praeobliquum, sample GM3.5 (GM3.5-NF/SK). 28, Gartnerago segmentatum,
- 1273 sample KA469.1 (KA469.1-NF/SK). 29, G. segmentatum, sample GM89 (GM89-NF/SK). 30-
- 1274 31, Gartnerago ponticula, sample GM89 (GM89-NF/SK). 32, G. ponticula, sample KA400,
- 1275 (KA400-NF/SK). 33–34, Gartnerago theta, sample GM56 (GM56-NF/SK). 35, Laguncula
- 1276 dorotheae, sample KA180 (KA180-NF/SK). 36, Laguncula cf. L. montrisouensis (top right),
- 1277 sample KA22.5 (KA22.5-NF/SK). 37, Repagulum parvidentatum, sample GM81.5 (GM81.5-
- 1278 NF/SK). 38–39, Calculites percernis, sample KA445.7 (KA445.7-NF/SK). 40–42, Calculites
- 1279 karaiensis, n. sp., sample KA459.3 (KA459.3-NF/SK).
- 1280
- 1281 Figure 8. Nannofossil species recorded in the Karai Fm., Karai and Garudamangalam sections
- 1282 (scale bar 2 µm). 1–2, *Calculites karaiensis*, n. sp., (1) HOLOTYPE, sample KA459.3
- 1283 (KA459.3-NF/SK). 3–5, C. karaiensis, n. sp., sample KA459.3 (KA459.3-NF/SK). 6–8, C.
- 1284 karaiensis, n. sp., (6) PARATYPE, sample KA459.3 (KA459.3-NF/SK). 9, Lapideacassis glans,
- 1285 sample KA428.5 (KA428.5-NF/SK). 10, Lapideacassis cf. L. cornuta, sample KA469.1
- 1286 (KA469.1-NF/SK). 11–12, *Lithraphidites acutus*, sample KA404.5 (KA404.5-NF/SK). 13,
- 1287 Lithraphidites carniolensis, sample KA368.5 (KA368.5-NF/SK). 14–15, Lithraphidites
- 1288 pseudoquadratus, sample GM102.5 (GM102.5-NF/SK). 16, Microrhabdulus belgicus, sample
- 1289 KA459.3 (KA459.3-NF/SK). 17, Microrhabdulus decoratus, sample KA 448.9 (KA448.9-
- 1290 NF/SK). 18, Eprolithus floralis, sample KA319 (KA319-NF/SK). 19, E. floralis, sample
- 1291 KA445.7 (KA445.7-NF/SK). 20, E. floralis, sample KA424 (KA424-NF/SK). 21, E. floralis
- 1292 (side view), sample KA305.5 (KA305.5-NF/SK). 22, Eprolithus spp. (side view), sample
- 1293 KA469.1 (KA469.1-NF/SK). 23, Eprolithus spp. (side view), sample KA459.3 (KA459.3-

- 1294 NF/SK). 24, Eprolithus octopetalus, sample KA448.9 (KA448.9-NF/SK). 25, E. octopetalus,
- 1295 sample KA464.2 (KA464.2-NF/SK). 26, Eprolithus moratus, sample KA451.9 (KA451.9-
- 1296 NF/SK). 27, E. moratus, sample KA464.2 (KA464.2-NF/SK). 28, Radiolithus planus, sample
- 1297 KA424 (KA424-NF/SK). 29, Radiolithus cf. R. planus, sample GM46 (GM46-NF/SK). 30,
- 1298 Quadrum octobrachium, sample KA448.9 (KA448.9-NF/SK). 31, Q. octobrachium, sample
- 1299 KA451.9 (KA451.9-NF/SK). 32–34, Quadrum eneabrachium, sample KA448.9 (KA448.9-
- 1300 NF/SK). 35, Hayesites albiensis, sample KA58.5 (KA58.5-NF/SK). 36–37, H. albiensis, sample
- 1301 KA63 (KA63-NF/SK). 38–39, Hayesites irregularis, sample KA4.5 (KA4.5-NF/SK). 40–42,
- 1302 Braarudosphaera cf. B. africana, sample GM28 (GM28-NF/SK).
- 1303
- Figure 9 (a). Summary of biostratigraphic zones and nannofossil/macrofossil events in the Karai
 Section, Cauvery Basin.
- 1306 Figure 9 (b). Summary of biostratigraphic zones and nannofossil/macrofossil events in the
- 1307 Garudamangalam Section, Cauvery Basin.
- 1308
- 1309 Figure 10. Age-depth plots showing approximate sedimentation rates of (a) Karai Section, (b).
- 1310 Garudamangalam Section, Cauvery Basin.
- 1311